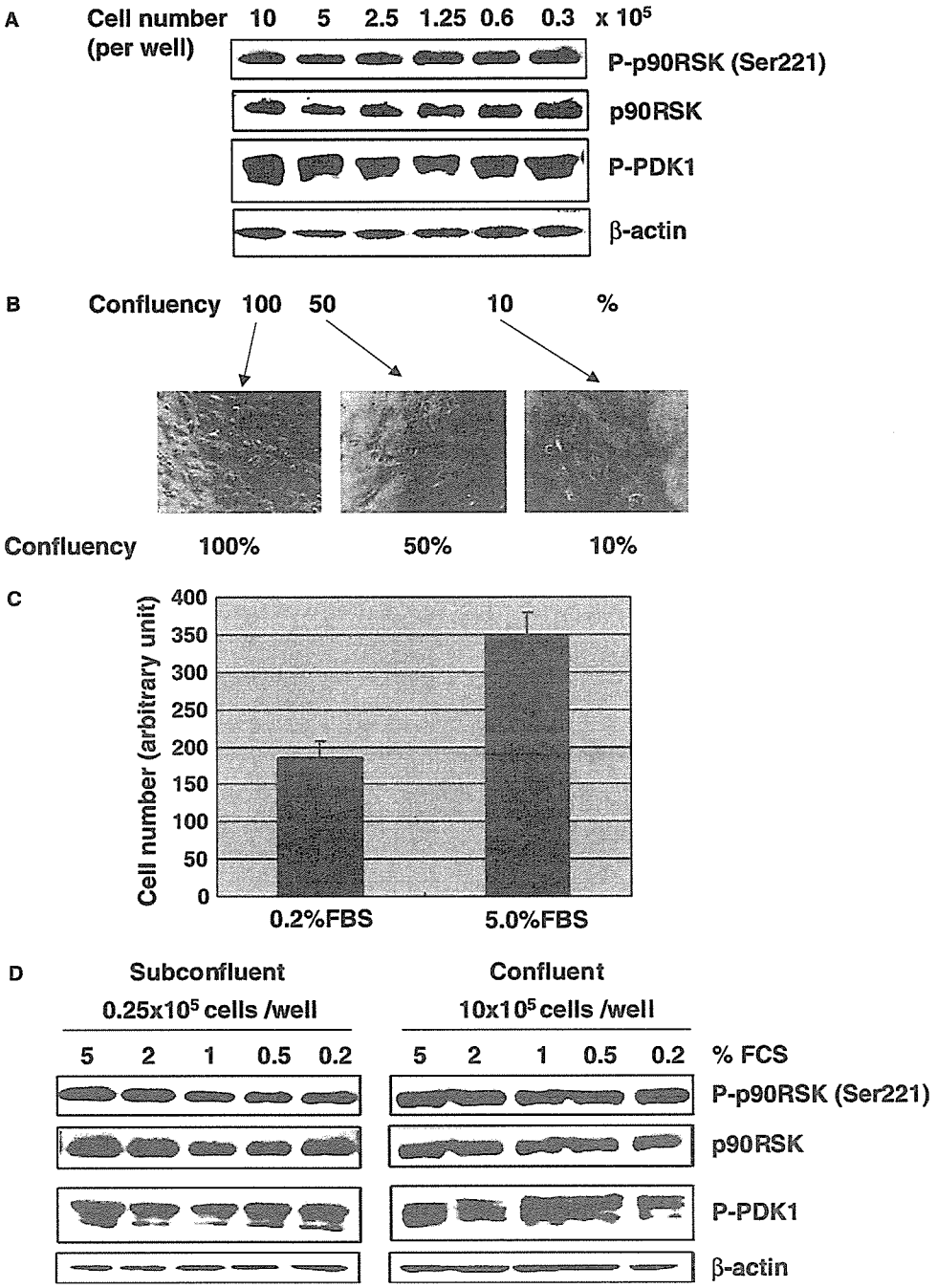

Fig. 3. Phosphorylation of p90RSK Ser221 in Vero E6 cells. (A) Vero E6 cells were prepared at densities of 10, 5, 2.5, 1.25, 0.6, and 0.3×10^5 cells in DMEM containing 5% FBS per well in 6-well plates. Proteins were obtained from these cells after 24 h, and Western blotting was performed using anti-phospho p90RSK (Ser221). (B) The confluency of Vero E6 cells used in this study is shown. (C) 2×10^3 cells in DMEM containing 0.2% and 5% FBS were prepared in 96-well plates. After 4 days, cell number was counted using a WST-1 cell proliferation assay kit. (D) 0.25 and 10×10^5 cells in DMEM containing various concentrations of FBS were prepared in 6-well plates. Western blotting was performed using proteins obtained after 24 h.

phosphorylation levels of PDK-1 and p90RSK Ser221 were unaffected by cell proliferation, Vero E6 cells were cultured in medium containing low and high concentrations of FBS. Cell proliferation of Vero E6 cells was partially suppressed in medium containing 0.2% FBS as compared with 5% FBS (Fig. 3C). Confluent and subconfluent cells in medium containing 5–0.2% FBS showed similar phosphorylation levels of PDK-1 and p90RSK at Ser221 (Fig. 3D). Thus, the phosphorylation level of Ser221 of p90RSK is not influenced by the status of cell proliferation.

3.3. Phosphorylation of p90RSK Ser380 and Thr573 in Vero E6 cells

p90RSK1 is phosphorylated at Thr573 in the activation loop of the C-terminal kinase domain [9,10], and this activation of the C-terminal kinase domain is thought to lead to autophosphorylation at Ser380 [11]. Activation of the C-terminal domain by the ERK signaling pathway is thought to be necessary for phosphorylation at Ser380 [34]. Fig. 4A indicates that EGF treatment induces phosphorylation of ERK in Vero E6 cells. Both Thr573 and Ser380 of p90RSK were phosphor-

ylated early after EGF treatment. Interestingly, the phosphorylation level of p90RSK Ser221 was not altered by EGF treatment. To investigate whether cell density affects phosphorylation level of p90RSK Thr573 and Ser380, Western blotting analysis was performed using proteins obtained from 10, 5, 2.5, 1.25, 0.6, and 0.3×10^5 cells in DMEM containing 5% FBS per well in 6-well plates. Fig. 4B shows that Ser380 of p90RSK phosphorylation was increased by decreasing cell density. Although Thr573 was also increased phosphorylation by decreasing cell density, the amount was very low. The amount of Thr573 phosphorylated p90RSK in 0.3×10^5 cells is only 11.53% of Ser380 using LAS-3000 mini system. Therefore, the band of Thr573 phosphorylated p90RSK was difficult to see in Fig. 4B.

3.4. Phosphorylation of p90RSK in SARS-CoV-infected cells

To investigate regulation of p90RSK phosphorylation in SARS-CoV-infected cells, confluent Vero E6 cells were infected with SARS-CoV at approximately 50 m.o.i., and Western blotting analysis was performed using proteins at 26 and 24 h.p.i. As shown in Fig. 5A, no significant differences in phosphorylation levels of PDK-1 or p90RSK at Ser221 were observed between confluent virus-infected cells at 16 and 24 h.p.i. Phosphorylation of Thr573 was not upregulated by viral infection. Ser380 of p90RSK is phosphorylated in virus-infected confluent cells. Previous reports indicated autophosphorylation of Ser380 after activation of C-terminal kinase domain [11]. Thus, phosphorylation of p90RSK Ser380 is upregulated without upregulation of Thr573 in SARS-CoV-infected cells.

3.5. Phosphorylation of p90RSK Ser380 under ERK and p38 MAPK signaling pathways

These observations raise a question regarding which signaling pathway regulates phosphorylation of Ser380 of p90RSK in SARS-CoV-infected cells. p90RSK is thought to act in response to stimulation and p38 MAPK plays key roles in cytopathic effects in SARS-CoV-infected cells, as shown in Fig. 1 and in our previous study [24]. As shown in Fig. 5A, Ser380 was phosphorylated without phosphorylation of Thr573 in virus-infected cells, suggesting that the ERK signaling pathway is not important for phosphorylation of Ser380. We next investigated whether p38 MAPK inhibitor can inhibit phosphorylation of Ser380. Confluent cells were prepared in 24-well plates. Cells were infected with SARS-CoV for 1 h, and then SB203580 was added as a p38 MAPK inhibitor. Western blotting analysis was performed using proteins at 24 h.p.i. As shown in Fig. 5B, phosphorylation of Ser380 was decreased in SB203580-treated cells.

4. Discussion

In the present study, we showed that p90RSK, the best-known substrate of ERK and PDK-1, was regulated phosphorylation in SARS-CoV-infected Vero E6 cells. There has been one previous report regarding phosphorylation of p90RSK by viral infection. Rous sarcoma virus has the ability to phosphorylate p90RSK [35], but there have been no detailed analyses of p90RSK phosphorylation. Investigation of the phosphorylation status of p90RSK by viral infection is

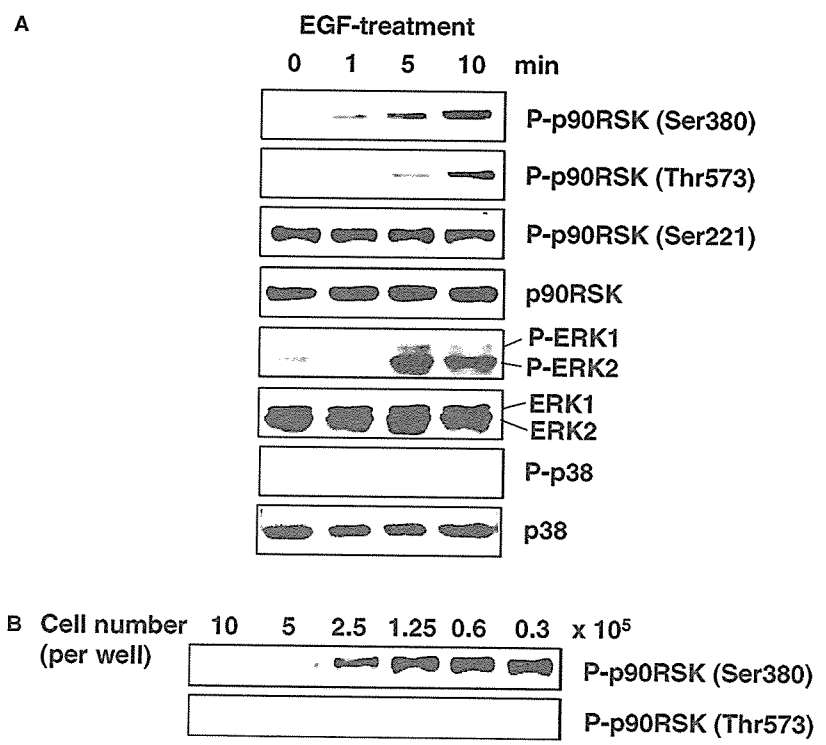

Fig. 4. Phosphorylation of p90RSK Thr573 and Ser380 in Vero E6 cells. Confluent Vero E6 cells in 24-well plates were treated with EGF. Western blotting analysis was performed using proteins obtained at 0, 1, 5, and 10 min (A). (B) Vero E6 cells were prepared at 10, 5, 2.5, 1.25, 0.6, and 0.3×10^5 cells in 6-well plates. Proteins were obtained from these cells after 24 h, and Western blotting was performed using anti-phospho p90RSK (Thr573 and Ser380). The proteins used in (B) were the same as those in Fig. 3A, and equal amount of proteins were blotted.

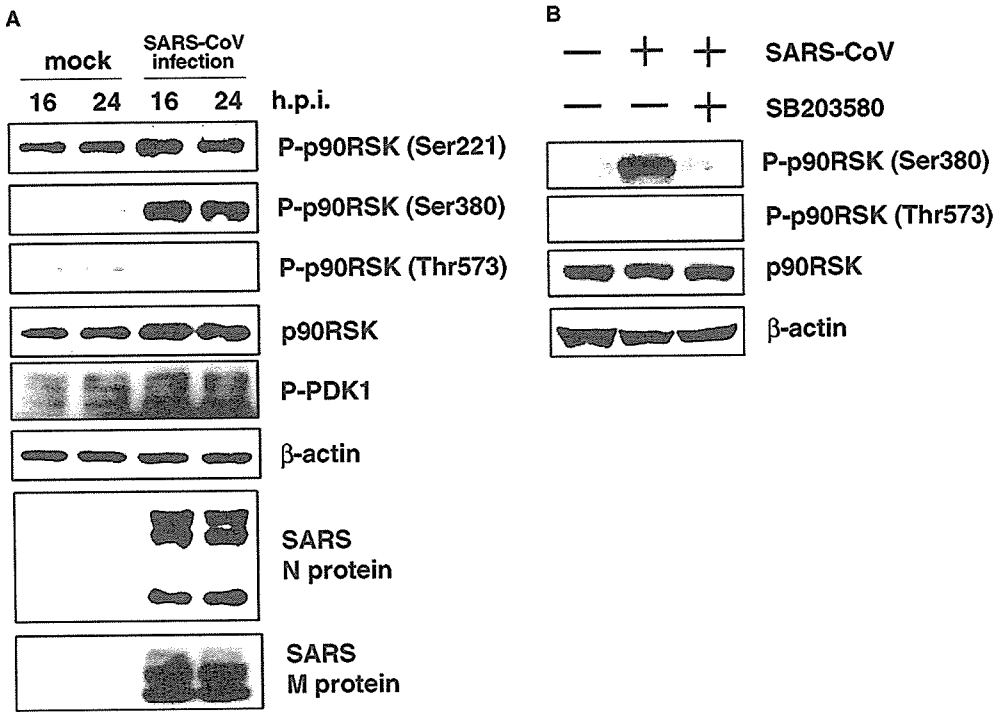

Fig. 5. Phosphorylation of p90RSK in SARS-CoV-infected Vero E6 cells. (A) 1×10^6 cells in 6-well plates were prepared (100% confluency). The cells were infected with SARS-CoV at 50 m.o.i. Western blotting analysis was performed using proteins obtained at 16 and 24 h.p.i. (B) One hour after viral inoculation, cells were treated with SB203580 (20 μM). Proteins were obtained at 24 h.p.i. for Western blotting analysis. Mock-infected cells were treated with DMSO as a control.

important as activation of p90RSK is involved in control of apoptosis.

Thr573 of p90RSK in mock infected cells was phosphorylated by EGF stimulation (Fig. 4A). The Thr573 was slightly phosphorylated in subconfluent mock infected cells compared with confluent mock infected cells (Fig. 4B). However, the phosphorylation was decreased by SARS-CoV-infection and was abolished by the MEK1/2-specific inhibitor, PD98059 (data not shown). Therefore, the ERK signaling pathway is involved in phosphorylation of Thr573 in Vero E6 cells. These observations raise a question regarding the role of ERK in SARS-CoV-infected cells. PD98059-treated SARS-CoV-infected Vero E6 cells showed no significant changes in activated caspase-3 or -7 at 18 h.p.i. (data not shown). This result suggested that phosphorylation of ERK was not sufficient to prevent apoptosis by SARS-CoV infection, as discussed previously regarding the lack of an inhibitory effect on apoptosis due to low activation of Akt in virus-infected cells [27]. Furthermore, we found different phosphorylation kinetics between ERK1 and ERK2 in EGF-treated and SARS-CoV-infected cells. Interestingly, the phosphorylation level of ERK1 is similar to that of ERK2 in SARS-CoV-infected Vero E6 cells (Fig. 1B). Among several experiments, the phosphorylation level of ERK1 was sometimes higher than that of ERK2, as in the case of virus-infected Vero cells at 27 and 44 h.p.i. (Fig. 1B). The total amounts of ERK1 were lower than those of total ERK2 in both mock- and SARS-CoV-infected cells. To confirm that factors contained in seed virus do not upregulate phosphorylation of ERK1, SARS-CoV in seed virus was completely neutralized by anti-SARS-CoV antibody, and then added to cells, resulting in no upregulation of the phosphorylation of ERK1/2 (data not shown). Thus, the strong phosphorylation of ERK1 occurred specifically in SARS-CoV-infected cells. In the case of EGF stimulation, the phosphorylation level of ERK1 was lower than that of ERK2 (Fig. 4A). Eblen et al. showed that ERK2 phosphorylates p90RSK [34]. Angenstein et al. identified p90RSK, ERK2, and GSK-3β as poly-associated proteins, suggesting that polyribosome-bound ERK2 activates p90RSK, and then inhibits GSK-3β [36]. Thus, ERK2 activation is important for phosphorylation of p90RSK in the absence of viral infection. On the other hand, the strong phoshorylation of ERK1 in SARS-CoV-infected cells may affect on phosphorylation status of p90RSK as discussed below.

p90RSK is phosphorylated at Thr573 in the activation loop of the C-terminal kinase domain, and then autophosphorylation at Ser380 in the linker region is thought to be led by this C-terminal kinase domain [11,40]. The phosphorylation level of Ser380 in confluent Vero E6 cells was very low, and SARS-CoV infection induced phosphorylation of Ser380 (Fig. 5). However, as described above, upregulation of Thr573 was not observed in virus-infected cells. There may be differences in regulation of Ser380 in SARS-CoV-infected cells from other stimuli. In the present study, we showed that p38 MAPK can induce phosphorylation of Ser380. Several reports have suggested that p90RSK activation results in phosphorylation of CREB [2,41]. Our previous study showed that SARS-CoV infection of Vero E6 cells induces phosphorylation of CREB, and treatment with SB203580 can inhibit this phosphorylation [24]. Thus, phosphorylation of CREB is regulated by p38 MAPK in SARS-CoV-infected cells. In addition, phosphorylation of ERKs was partially downregulated by treatment with SB203580 in virus-infected cells in viral infected cells (data not shown). Although there is a possibility of

nonspecific reaction by SB203580, cross-talk between ERK and p38 has been reported [37–39]. On the other hand, EGF stimulation induces phosphorylation of ERK without phosphorylation of p38 MAPK (Fig. 4A). Several signaling pathways of p38 MAPK and ERKs including cross-talk may exist in Vero E6 cells. These results may indicate a signaling cascade, p38 MAPK > (ERK >) p90RSK > CREB, in virus-infected cells. Further investigations are necessary to clarify the roles of p90RSK in virus-infected cells.

Based on these results, we conclude that phosphorylation of p90RSK Ser380 is regulated by p38 MAPK, in the absence of upregulation of Thr573 phosphorylation in SARS-CoV-infected cells. These new observations provide valuable insights into the biological effects of p90RSK in SARS-CoV infection.

Acknowledgements: We thank Dr. Funaba (Azabu University, Japan) for helpful suggestions. We also thank Ms. M. Ogata (National Institute of Infectious Diseases, Japan) for her assistance. This work was supported in part by the Japan Health Science Foundation and Grants-in-Aid for Scientific Research, Tokyo, Japan.

References

[1] Pearson, G., Robinson, F., Beers Gibson, T., Xu, B.E., Karandikar, M., Berman, K. and Cobb, M.H. (2001) Mitogen-activated protein (MAP) kinase pathways: regulation and physiological functions. Endocr. Rev. 22, 153–183.

[2] Frodin, M. and Gammeltoft, S. (1999) Role and regulation of 90 kDa ribosomal S6 kinase (RSK) in signal transduction. Mol. Cell. Endocrinol. 151, 65–77.

[3] Moller, D.E., Xia, C.H., Tang, W., Zhu, A.X. and Jakubowski, M. (1994) Human rsk isoforms: cloning and characterization of tissue-specific expression. Am. J. Physiol. 266, C351–C359.

[4] Zhao, Y., Bjorbaek, C., Weremowicz, S., Morton, C.C. and Moller, D.E. (1995) RSK3 encodes a novel pp90rsk isoform with a unique N-terminal sequence: growth factor-stimulated kinase function and nuclear translocation. Mol. Cell. Biol. 15, 4353–4363.

[5] Yntema, H.G., van den Helm, B., Kissing, J., van Duijnhoven, G., Poppelaars, F., Chelly, J., Moraine, C., Fryns, J.P., Hamel, B.C., Heilbronner, H., Pander, H.J., Brunner, H.G., Ropers, H.H., Cremers, F.P. and van Bokhoven, H. (1999) A novel ribosomal S6-kinase (RSK4; RPS6KA6) is commonly deleted in patients with complex X-linked mental retardation. Genomics 62, 332–343.

[6] Bjorbeak, C., Zhao, Y. and Moller, D.E. (1995) Divergent functional roles for p90RSK kinase domains. J. Biol. Chem. 270, 18848–18852.

[7] Fisher, T.L. and Blenis, J. (1996) Evidence for two catalytically active kinase domains in pp90rsk. Mol. Cell. Biol. 16, 1212–1219.

[8] Vik, T.A. and Ryder, J.W. (1997) Identification of serine 380 as the major site of autophosphorylation of xenopus pp90rsk. Biochem. Biophys. Res. Commun. 235, 398–402.

[9] Gavin, A.C. and Nebreda, A.R. (1999) A MAP kinase docking site is required for phosphorylation and activation of $p90^{rsk}$/MAPKAP kinase-1. Curr. Biol. 9, 281–284.

[10] Smith, J.A., Poteet-Smith, C.E., Malarkey, K. and Sturgill, T.W. (1999) Identification of an extracellular signal-regulated kinase (ERK) docking site in ribosomal S6 kinase, a sequence critical for activation by ERK in vivo. J. Biol. Chem. 274, 2893–2898.

[11] Vik, T.A., Sweet, L.J. and Erikson, R.L. (1990) Coinfection of insect cells with recombinant baculovirus expressing pp60v-src results in the activation of a serine-specific protein kinase pp90rsk. Proc. Natl. Acad. Sci. USA 87, 2685–2689.

[12] Frödin, M., Jensen, C.J., Merienne, K. and Gammeltoft, S. (2000) A phosphoserine-regulated docking site in the protein kinase RSK2 that recruits and activates PDK1. EMBO J. 19, 2924–2934.

[13] Jensen, C.J., Buch, M.B., Krag, T.O., Hemmings, B.A., Gammeltoft, S. and Frodin, M. (1999) 90-kDa ribosomal S6 kinase is phosphorylated and activated by 3-phosphoinositide-dependent protein kinase-1. J. Biol. Chem. 274, 27168–27176.

[14] Richards, S.A., Fu, J., Romanelli, A., Shimamura, A. and Blenis, J. (1999) Ribosomal S6 kinase 1 (RSK1) activation requires signals dependent on and independent of the MAP kinase ERK. Curr. Biol. 9, 810–820.

[15] Bonni, A., Brunet, A., West, A.E., Datta, S.R., Takasu, M.A. and Greenberg, M.E. (1999) Cell survival promoted by the Ras-MAPK signaling pathway by transcription-dependent and -independent mechanisms. Science 286, 1358–1362.

[16] Dalby, K.N., Morrice, N., Caudwell, F.B., Avruch, J. and Cohen, P. (1988) Identification of regulatory phosphorylation sites in mitogenactivated protein kinase (MAPK)-activated protein kinase-1a/p90rsk that are inducible by MAPK. J Biol. Chem. 273, 1496–1505.

[17] Buck, M., Poli, V., Hunter, T. and Chojkier, M. (2001) C/EBPβ phosphorylation by RSK creates a functional XEXD caspase inhibitory box critical for cell survival. Mol. Cell 8, 807–816.

[18] Palmer, A., Gavin, A.C. and Nebreda, A.R. (1998) A link between MAP kinase and $p34^{cdc2}$/cyclin B during oocyte maturation: $p90^{rsk}$ phosphorylates and inactivates the $p34^{cdc2}$ inhibitory kinase Myt1. EMBO J. 17, 5037–5047.

[19] Chun, J., Chau, A.S., Maingat, F.G., Edmonds, S.D., Ostergaard, H.L. and Shibuya, E.K. (2005) Phosphorylation of Cdc25C by pp90Rsk contributes to a G2 cell cycle arrest in *Xenopus* cycling egg extracts. Cell Cycle 4, 148–154.

[20] Paronetto, M.P., Giorda, E., Carsetti, R., Rossi, P., Geremia, R. and Sette, C. (2004) Functional interaction between $p90^{Rsk2}$ and Emilcontributes to the metaphase arrest of mouse oocytes. EMBO J. 23, 4649–4659.

[21] Itoh, S., Ding, B., Bains, C.P., Wang, N., Takeishi, Y., Jalili, T., King, G.L., Walsh, R.A., Yan, C. and Abe, J. (2005) Role of p90 ribosomal S6 kinase (p90RSK) in reactive oxygen species and protein kinase Cβ (PKC-β)-mediated cardiac troponin I phosphorylation. J. Biol. Chem. 280, 24135–24142.

[22] Marra, M.A., Jones, S.J., Astell, C.R., Holt, R.A., Brooks-Wilson, A., Butterfield, Y.S., Khattra, J., Asano, J.K., Barber, S.A., Chan, S.Y., Cloutier, A., Coughlin, S.M., Freeman, D., Girn, N., Griffith, O.L., Leach, S.R., Mayo, M., McDonald, H., Montgomery, S.B., Pandoh, P.K., Petrescu, A.S., Robertson, A.G., Schein, J.E., Siddiqui, A., Smailus, D.E., Stott, J.M., Yang, G.S., Plummer, F., Andonov, A., Artsob, H., Bastien, N., Bernard, K., Booth, T.F., Bowness, D., Czub, M., Drebot, M., Fernando, L., Flick, R., Garbutt, M., Gray, M., Grolla, A., Jones, S., Feldmann, H., Meyers, A., Kabani, A., Li, Y., Normand, S., Stroher, U., Tipples, G.A., Tyler, S., Vogrig, R., Ward, D., Watson, B., Brunham, R.C., Krajden, M., Petric, M., Skowronski, D.M., Upton, C. and Roper, R.L. (2003) The genome sequence of the SARS-associated coronavirus. Science 300, 1399–1404.

[23] Rota, P.A., Oberste, M.S., Monroe, S.S., Nix, W.A., Campagnoli, R., Icenogle, J.P., Penaranda, S., Bankamp, B., Maher, K., Chen, M.H., Tong, S., Tamin, A., Lowe, L., Frace, M., DeRisi, J.L., Chen, Q., Wang, D., Erdman, D.D., Peret, T.C., Burns, C., Ksiazek, T.G., Rollin, P.E., Sanchez, A., Liffick, S., Holloway, B., Limor, J., McCaustland, K., Olsen- Rasmussen, M., Fouchier, R., Gunther, S., Osterhaus, A.D., Drosten, C., Pallansch, M.A., Anderson, L.J. and Bellini, W.J. (2003) Characterization of a novel coronavirus associated with severe acute respiratory syndrome. Science 300, 1394–1399.

[24] Mizutani, T., Fukushi, S., Saijo, M., Kurane, I. and Morikawa, S. (2004) Phosphorylation of p38 MAPK and its downstream targets in SARS coronavirus-infected cells. Biochem. Biophys. Res. Commun. 319, 1228–1234.

[25] Mizutani, T., Fukushi, S., Murakami, M., Hirano, T., Saijo, M., Kurane, I. and Morikawa, S. (2004) Tyrosine dephosphorylation of STAT3 in SARS coronavirus-infected Vero E6 cells. FEBS Lett. 577, 187–192.

[26] Mizutani, T., Fukushi, S., Saijo, M., Kurane, I. and Morikawa, S. (2005) JNK and PI3k/Akt signaling pathways are required for establishing persistent SARS-CoV infection in Vero E6 cells. Biochem. Biophys. Acta 1741, 4–10.

[27] Mizutani, T., Fukushi, S., Saijo, M., Kurane, I. and Morikawa, S. (2004) Importance of Akt signaling pathway for apoptosis in SARS-CoV-infected Vero E6 cells. Virology 327, 169–174.

[28] Watanabe, H., de Caestecker, M.P. and Yamada, Y. (2001) Transcriptional cross-talk between Smad, ERK1/2, and p38

mitogen-activated protein kinase pathways regulates transforming growth factor-beta-induced aggrecan gene expression in chondrogenic ATDC5 cells. J. Biol. Chem. 276, 14466–14473.
[29] Surjit, M., Liu, B., Jameel, S., Chow, V.T. and Lal, S.K. (2004) The SARS coronavirus nucleocapsid protein induces actin reorganization and apoptosis in COS-1 cells in the absence of growth factors. Biochem. J. 383, 13–18.
[30] He, R., Leeson, A., Andonov, A., Li, Y., Bastien, N., Cao, J., Osiowy, C., Dobie, F., Cutts, T., Ballantine, M. and Li, X. (2003) Activation of AP-1 signal transduction pathway by SARS coronavirus nucleocapsid protein. Biochem. Biophys. Res. Commun. 311, 870–876.
[31] Tan, Y.J., Fielding, B.C., Goh, P.Y., Shen, S., Tan, T.H., Lim, S.G. and Hong, W. (2004) Overexpression of 7a, a protein specifically encoded by the severe acute respiratory syndrome coronavirus, induces apoptosis via a caspase-dependent pathway. J. Virol. 78, 14043–14047.
[32] Chang, Y.J., Liu, C.Y., Chiang, B.L., Chao, Y.C. and Chen, C.C. (2004) Induction of IL-8 release in lung cells via activator protein-1 by recombinant baculovirus displaying severe acute respiratory syndrome-coronavirus spike proteins: identification of two functional regions. J. Immunol. 173, 7602–7614.
[33] Zeniou, M., Ding, T., Trivier, E. and Hanauer, A. (2002) Expression analysis of RSK gene family members: the RSK2 gene, mutated in Coffin–Lowry syndrome, is prominently expressed in brain structures essential for cognitive function and learning. Hum. Mol. Genet. 11, 2929–2940.
[34] Eblen, S.T., Catling, A.D., Assanah, M.C. and Weber, M.J. (2001) Biochemical and biological functions of the N-terminal, noncatalytic domain of extracellular signal-regulated kinase 2. Mol. Cell. Biol. 21, 249–259.
[35] Wang, H.C. and Erikson, R.L. (1992) Activation of protein serine/threonine kinases p42, p63, and p87 in Rous sarcoma virus-transformed cells: signal transduction/transformation-dependent MBP kinases. Mol. Biol. Cell. 3, 1329–1337.
[36] Angenstein, F., Greenough, W.T. and Weiler, I.J. (1998) Metabotropic glutamate receptor-initiated translocation of protein kinase p90rsk to polyribosomes: a possible factor regulating synaptic protein synthesis. Proc. Natl. Acad. Sci. USA 95, 15078–15083.
[37] Xiao, Y.Q., Malcolm, K., Worthen, G.S., Gardai, S., Schiemann, W.P., Fadok, V.A., Bratton, D.L. and Henson, P.M. (2002) Cross-talk between ERK and p38 MAPK mediates selective suppression of pro-inflammatory cytokines by transforming growth factor-β. J. Biol. Chem. 277, 14884–14893.
[38] Mizutani, T., Fukushi, S., Iizuka, D., Inanami, O., Kuwabara, M., Takashima, H., Yanagawa, H., Saijo, M., Kurane, I. and Morikawa, S. Inhibition of cell proliferation by SARS-CoV infection in Vero E6 cells. FEMS Immunol. Med. Microbiol. (in press).
[39] Houliston, R.A., Pearson, J.D. and Wheeler-Jones, C.P.D. (2001) Agonist-specific cross talk between ERKs and $p38^{mapk}$ regulates PGI_2 synthesis in endothelium. Am. J. Physiol. Cell Physiol. 281, C1266–C1276.
[40] Grove, J.R., Price, D.J., Banerjee, P., Balasubramanyam, A., Ahmad, M.F. and Avruch, J. (1993) Regulation of an epitope-tagged recombinant Rsk-1 S6 kinase by phorbol ester and erk/MAP kinase. Biochemistry 32, 7727–7738.
[41] Böhm, M., Moellmann, G., Cheng, E., Alvarez-Franco, M.S.W. and Sassone-Corsi, P.R.H. (1955) Identification of p90RSK as the probable CREB-Ser133 kinase in human melanocytes. Cell Growth Differ. 6, 291–302.

Journal of Medical Virology 78:954–963 (2006)

Protection Against Influenza Virus Infection by Intranasal Vaccine with Surf Clam Microparticles (SMP) as an Adjuvant

Takeshi Ichinohe,[1,2] Izumi Watanabe,[1,2] Eriko Tao,[1] Satoshi Ito,[1,2] Akira Kawaguchi,[1,2] Shin-ichi Tamura,[1] Hidehiro Takahashi,[1] Hirofumi Sawa,[3] Masami Moriyama,[4] Joe Chiba,[2] Katsuhiro Komase,[5] Yujiro Suzuki,[5] Takeshi Kurata,[1] Tetsutaro Sata,[1] and Hideki Hasegawa[1]*

[1]*Department of Pathology, National Institute of Infectious Diseases, Tokyo, Japan*
[2]*Department of Biological Science and Technology, Tokyo University of Science, Chiba, Japan*
[3]*Department of Molecular Pathobiology and 21st Century COE Program for Zoonosis Control, Hokkaido University Research Center for Zoonosis Control, Sapporo, Japan*
[4]*Department of Microbiology and Immunology, School of Medicine, Keio University, Tokyo, Japan*
[5]*Research Center for Biologicals, Kitasato Institute, Kitamoto, Saitama, Japan*

A safe and effective adjuvant is necessary to enhance mucosal immune responses for the development of an inactivated intranasal influenza vaccine. The present study demonstrated the effectiveness of surf clam microparticles (SMP) derived from natural surf clams as an adjuvant for an intranasal influenza vaccine. The adjuvant effect of SMP was examined when co-administered intranasally with inactivated A/PR8 (H1N1) influenza virus hemagglutinin vaccine in BALB/c mice. Administration of the vaccine with SMP induced a high anti-PR8 haemagglutinin (HA)-specific immunoglobulin A (IgA) response in the nasal wash and immunoglobulin G (IgG) response in the serum, resulting in protection against both nasal-restricted infection and lethal lung infection by A/PR8 virus. In addition, administration of SMP with A/Yamagata (H1N1), A/Beijing (H1N1), or A/Guizhou (H3N2) vaccine conferred complete protection against A/PR8 virus challenge in the nasal infection model, suggesting that SMP adjuvanted vaccine can confer cross-protection against variant influenza viruses. The use of SMP is suggested as a new safe and effective mucosal adjuvant for nasal vaccination against influenza virus infection. ***J. Med. Virol. 78:954–963, 2006.*** © 2006 Wiley-Liss, Inc.

KEY WORDS: influenza; surf clams; natural adjuvant; nasal vaccine; IgA

INTRODUCTION

Influenza virus causes annual epidemics of the serious infectious disease, influenza. Lethal pneumonia and encephalopathy caused by influenza virus have now become a serious problem in Japan, especially among children and the elderly [Smidt et al., 2004; Wada, 2004]. Inactivated split vaccines against the influenza virus have been administered parenterally to induce serum anti-HA immunoglobulin G (IgG) antibodies (Abs), which are highly protective against homologous virus infection, but are less effective against heterologous virus infection [Tamura and Kurata, 1997]. There have been many studies, including the use of intranasal vaccination, to resolve this issue with lack of cross-protection [Jackson et al., 1999; Piedra et al., 2002; Watanabe et al., 2002, 2003; Hasegawa et al., 2005]. A large number of studies have shown that the mucosal immunity acquired by natural infection, which is due mainly to the secreted form of immunoglobulin A (IgA; s-IgA) in the respiratory tract, is more effective and cross protective against virus infection than the systemic immunity induced by parenteral vaccines in humans and mice [Tamura and Kurata, 2000]. In this regard, induction of s-IgA in the respiratory tract is advanta-

Abbreviations used: HA, haemagglutinin; IgA, immunoglobulin A; IgG, immunoglobulin G; Abs, antibodies; s-IgA, secreted form of IgA; CT, cholera toxin; LT, *Escherichia coli* heat-labile toxin; HI, haemagglutination inhibition; CTB*, cholera toxin B subunits containing a trace amount of holotoxin; CMP, chitin microparticles; poly(I:C), polyriboinosinic-polyribocytidylic acid; PFU, plaque-forming unit; MDCK, Madin–Darby canine kidney; APC, antigen-presenting cells; SMP, surf clam microparticles; i.c., intracerebral; i.p., intraperitoneal; i.n., intranasal; i.g., intragastric.

Grant sponsor: Ministry of Health, Labour and Welfare and Research on Health Sciences focusing on Drug Innovation.

*Correspondence to: Hideki Hosegawa, Department of Pathology, National Institute of Infectious Diseases, 4-7-1 Gakuen, Musashimurayama-shi, Tokyo 208-0011, Japan.
E-mail: hasegawa@nih.go.jp

Accepted 30 March 2006
DOI 10.1002/jmv.20647
Published online in Wiley InterScience (www.interscience.wiley.com)

geous with regard to protection against unpredictable epidemics of influenza.

In developing intranasal vaccines, cholera toxin (CT) and *Escherichia coli* heat-labile toxin (LT) have been used as adjuvants to enhance mucosal immune responses [Tamura and Kurata, 2000]. Although CT and LT are effective adjuvants to induce mucosal immune responses, they have some side effects in humans, such as nasal discharge [van Ginkel et al., 2000; Mutsch et al., 2004]. Therefore, other adjuvants that are as effective as CT or LT and are also safe for human use have been developed for clinical application with intranasal influenza vaccine, such as ISCOMATRIX, chitin microparticles (CMP), mutant CT, complement C3d, and synthetic double-stranded RNA [polyriboinosinic-polyribocytidylic acid (poly(I:C))] [Watanabe et al., 2002, 2003; Coulter et al., 2003; Hasegawa et al., 2005; Ichinohe et al., 2005]. In a screen for materials that can act as vaccine carriers to the nasal mucosa, the safety and effectiveness of the natural shell-derived surf clam microparticles (SMP) as an immune-enhancing adjuvant in comparison with other adjuvants, such as cholera toxin B subunits containing a trace amount of holotoxin (CTB*), poly(I:C), and CMP was demonstrated. The antigen particle size is important to obtain an immune response, as the particles must be engulfed by antigen-presenting cells (APC). Surf clam microparticles, which consist of 98.9% calcium micro-powder of fired natural surf clams and have particles 1–10 μm in diameter, are a good candidate as a vaccine carrier because of the size and surface features of the microparticles.

The results of the present study demonstrated the mucosal adjuvant effect and the induction of cross-protective immune responses against homologous and heterologous influenza variants by intranasal administration of inactivated influenza haemagglutinin (HA) vaccine together with SMP.

MATERIALS AND METHODS

Mice

Female BALB/c mice (Shizuoka Agricultural Cooperative Association for Laboratory Animals, Hamamatsu, Japan), 6–8 weeks old at the time of immunization, were used in all experiments. All animal experiments were carried out in accordance with the Guides for Animal Experiments Performed at NIID and were approved by the Animal Care and Use Committee of the National Institute of Infectious Diseases.

HA Vaccines and Influenza Viruses

HA vaccines (split-product virus vaccines) were prepared from the family Orthomyxoviridae, genus *Influenzavirus A,B*, species *Influenzavirus A*, including A/PuertoRico/3/334 (A/PR8; H1N1), A/Yamagata/120/86 (A/Yamagata; H1N1), A/Beijing/262/95 (A/Beijing; H1N1), A/Guizhou/54/89 (A/Guizhou, H3N2), and B/Ibaraki/2/85 (B/Ibaraki) strains, according to the method of Davenport et al. [1964] at the Kitasato Institute (Saitama, Japan). These viruses were grown in the allantoic cavities of 10–11-day fertile chicken eggs, purified and disintegrated with ethyl ether. The vaccines contained all proteins from the virus particle; however, the major component of the vaccine was HA (about 30% of the total protein). The PR/8 virus used for the challenge experiments was adapted to mice by subculturing 148 times in ferret, 596 times in mouse, and 73 times in 10-day fertile chicken eggs.

Preparation of Adjuvants

Fired surf clam shells were ground into microparticles about 10 μm in diameter by Daido Sangyo (Tokyo, Japan) and provided as SMP. Cholera toxin B subunits containing a trace amount of holotoxin (CTB*) were prepared by adding 0.1% CT (holotoxin) to CTB (Sigma, St. Louis, MO). Synthetic double-stranded poly(I:C) RNA was kindly provided by Toray Industries, Inc. (Kamakura, Japan). Chitin microparticles (CMP) were prepared as described previously [Hasegawa et al., 2005].

Immunization and Infection

Five mice in each experimental group were anaesthetized with diethyl ether and primarily immunized intranasally (i.n.) by dropping 3 μg of HA vaccines with various adjuvants [SMP, CTB*, poly(I:C), or CMP] into each nostril. To examine the cross-reactivity of vaccinated mice against the variant influenza virus subtypes, doses of 3 μg of these HA vaccines were administered with 100 μg of SMP. Immunization was repeated at 3 and 5 weeks. For virus infection, two conditions regarding the site of infection were used according to a modification of the procedure of Yetter et al. [1980] [Tamura et al. [1996, 1998]. Under the first of these conditions, each mouse was anaesthetized and then infected by i.n. application of 20 μl of virus suspension (1,000 plaque-forming unit (PFU) in PBS; 40 LD_{50}). This procedure induced total respiratory tract infection, which resulted in virus shedding from the nose and lungs, and led to death from viral pneumonia about 7 days later. Under the other infection conditions, anaesthetized mice were infected by dropping 1 μl of virus suspension (1,000 PFU in PBS) into each nostril. The nasal-restricted volume (2 μl) of virus suspension induced localized infection in the nose, which was not lethal. The nasal and lung wash virus titers were used as indices of protection in the upper and lower respiratory tracts of immunized mice, respectively.

Measurement of Virus Titer and Anti-PR8 HA Antibodies

Serum, nasal wash, and bronchoalveolar wash were collected for measurement of virus titer and antibodies against PR8 HA from mice sacrificed under anesthesia with chloroform. To collect nasal wash, a hypodermic needle was inserted into the posterior opening of the

nasopharynx and 1 ml of PBS containing 0.1% BSA was injected three times. Bronchoalveolar wash was collected by washing the trachea and lungs twice by injecting a total of 2 ml PBS containing 0.1% BSA. The levels of IgA and IgG Abs against HA molecules purified from the A/PR8 viruses were determined by ELISA as described previously [Tamura et al., 1992]. Briefly, ELISA was performed sequentially from the solid phase (EIA plates; Costar, Cambridge, MA) with a ladder of reagents as follows: first, HA molecules purified from the A/PR8 virus according to the procedure of Phelan et al. [1980]; second, nasal wash, bronchoalveolar wash or serum; third, either goat anti-mouse IgA Ab (α-chain specific; Amersham, Piscataway, NJ) or goat anti-mouse IgG Ab (γ-chain-specific; Amersham) conjugated with biotin; fourth, streptavidin conjugated with alkaline phosphatase (Life Technologies, Rockville, MD); and fifth, *p*-nitrophenylphosphate. The chromogen produced was determined by measuring the absorbance at 405 nm using an ELISA reader. A twofold serial dilution of either purified HA-specific IgA (320 ng/ml) or HA-specific monoclonal IgG (160 ng/ml) was used as a standard as described previously [Asahi et al., 2002]. The binding kinetics of the standard HA-specific monoclonal IgG were comparable with HA-specific IgG from immunized mice. The Ab concentrations of unknown specimens were determined from the standard regression curves constructed for each assay with a programmed SJeia Autoreader (model er-8000; Sanko Junyaku, Tokyo, Japan).

Before the haemagglutination inhibition (HI) tests, receptor-destroying enzyme (RDE(II); Denka Seiken Co. Ltd., Tokyo, Japan) was added to the RBC-treated sera to inactivate non-specific haemagglutination inhibitors at 37°C overnight followed by incubation at 56°C for 1 hr to inactivate RDE. HI tests were performed according to the microtiter method of Sever [Sever, 1962]. Briefly, aliquots of 25 μl of serial twofold dilutions of the treated serum samples were mixed with 4HA units of virus in microtiter plates and incubated at room temperature for 30 min. Then, 50 μl of 0.5% chicken RBCs was added to each well and incubated at room temperature for 30–40 min. The HI titer was expressed as the reciprocal of the highest serum dilution that completely inhibited haemagglutination of 4HA units of the virus.

Virus neutralization by antisera was determined as described previously. Briefly, virus was mixed with antisera from naïve or vaccinated mice at 37°C for 1 hr, and the mixture was added to MDCK cells in a total volume of 200 μl. The neutralizing capacity of antisera was measured by comparing the reduction in number of infected cells per sample to sera from age-matched naïve control mice. Inhibition of virus was estimated by the additional reduction in infectivity beyond the background of naïve mouse antisera. Inhibition was measured by 50% inhibition of virus infection (beyond non-specific inhibition). Samples were run in duplicate assays on the same day and averaged, and data are presented as the average per group.

The virus titer was measured as follows: aliquots of 200 μl of serial 10-fold dilutions of the nasal wash by PBS containing 0.1% BSA were inoculated into Madin–Darby canine kidney (MDCK) cells in 6-well plates. After 1-hr incubation, each well was overlaid with 2 ml of agar medium according to the method of Tobita and coworkers [Tobita, 1975; Tobita et al., 1975]. The number of plaques in each well was counted 2 days after inoculation. All the experiments were repeated independently at least three times, and the data are presented as means ± SD.

Antigen-Specific T-Cell Response

Antigen-specific T-cell responses were measured as described previously [Takasuka et al., 2004]. Spleens were harvested from mice at 1 week after booster vaccination. After preparation of a single-cell suspension, T-cells were purified by depletion of $CD11b^+$ (Mac-1), $CD45R^+$ (B220), $DX5^+$, and $Ter\text{-}119^+$ cells using a magnetic cell sorter (MACS: Militenyi Biotec, Bergisch, Germany). To prepare APC, splenocytes from normal BALB/c mice were depleted of CD90 $(Thy1.2)^+$ cells by MACS and irradiated at 2000 cGy.

T-cells were purified from the spleen (1×10^5 cells/well) and cultured with irradiated APC (5×10^5 cells/well) in the presence or absence of PR8 vaccine (0.1 or 1.0 μg/ml). After 4 days of cultivation, the cytokine concentration in the culture supernatant was measured by ELISA using a Mouse IFN-γ Immunoassay Kit (Biosource International, Camarillo, CA) according to the manufacturer's instructions. T-cell proliferation was monitored by measuring the incorporation of $[^3H]$ thymidine (18.5 kBq/well; ICN Biomedicals, Costa Mesa, CA) added 8 hr prior to harvesting the cells on 96-well microplates bonded with a GF/B filter (Packard Instruments, Meriden, CT). Incorporated radioactivity was counted using a microplate scintillation counter (Packard Instruments).

Intracerebral, Intraperitoneal, Intranasal, and Intragastric Administration of Surf Clam Microparticles

Seven-week-old female BALB/c mice were injected intracerebrally with 250 μg of SMP in 25 μl of PBS or intraperitoneally with 1 mg of SMP in 100 μl of PBS once. Intranasal (i.n.) and intragastric (i.g.) administration were performed daily for 23 days with 100 μg or 1 mg of SMP, respectively, and mortality and body weight were monitored daily. PBS was used as a negative control.

Histopathological Examination

Excised nasal tissues were fixed with 10% neutral-buffered formalin, and decalcified in EDTA solution. After fixation, tissues were embedded in paraffin by conventional methods and stained with haematoxylin and eosin (H&E).

Statistical Analysis

Comparisons between experimental groups were performed by Student's t-test. $P < 0.05$ was considered significant.

RESULTS

Antibody Responses and Protective Efficacy Against Influenza Virus Infection in BALB/c Mice Immunized Intranasally With Vaccine and Surf Clam Microparticles as an Adjuvant

The effects of SMP as an adjuvant of intranasal influenza vaccine (A/PR8 strain) on protection against A/PR8 influenza virus infection were investigated in BALB/c mice. The mice were immunized three times intranasally with 3 μg of HA vaccine with various adjuvants [SMP, CTB*, poly(I:C), or CMP] to compare the activities of adjuvant candidates for mucosal application.

The concentrations of anti-A/PR8 HA IgA in the nasal wash, anti-HA IgG in the serum, anti-A/PR8 virus titer in the nasal wash, and titers of neutralizing antibodies of the immunized mice are summarized in Figure 1. High concentrations of mucosal IgA and serum IgG Abs were observed in mice treated with CTB*- and poly(I:C)-adjuvanted vaccines (Fig. 1A). Mice immunized with SMP-adjuvanted vaccine developed sufficient levels of specific Abs to confer protection against nasal-restricted influenza virus infection similar to those immunized with CMP-adjuvanted vaccine (Fig. 1A). There were no detectable levels of specific antibody in control mice immunized with non-adjuvanted vaccine or in non-immunized mice that were not protected against experimental infection (Fig. 1A).

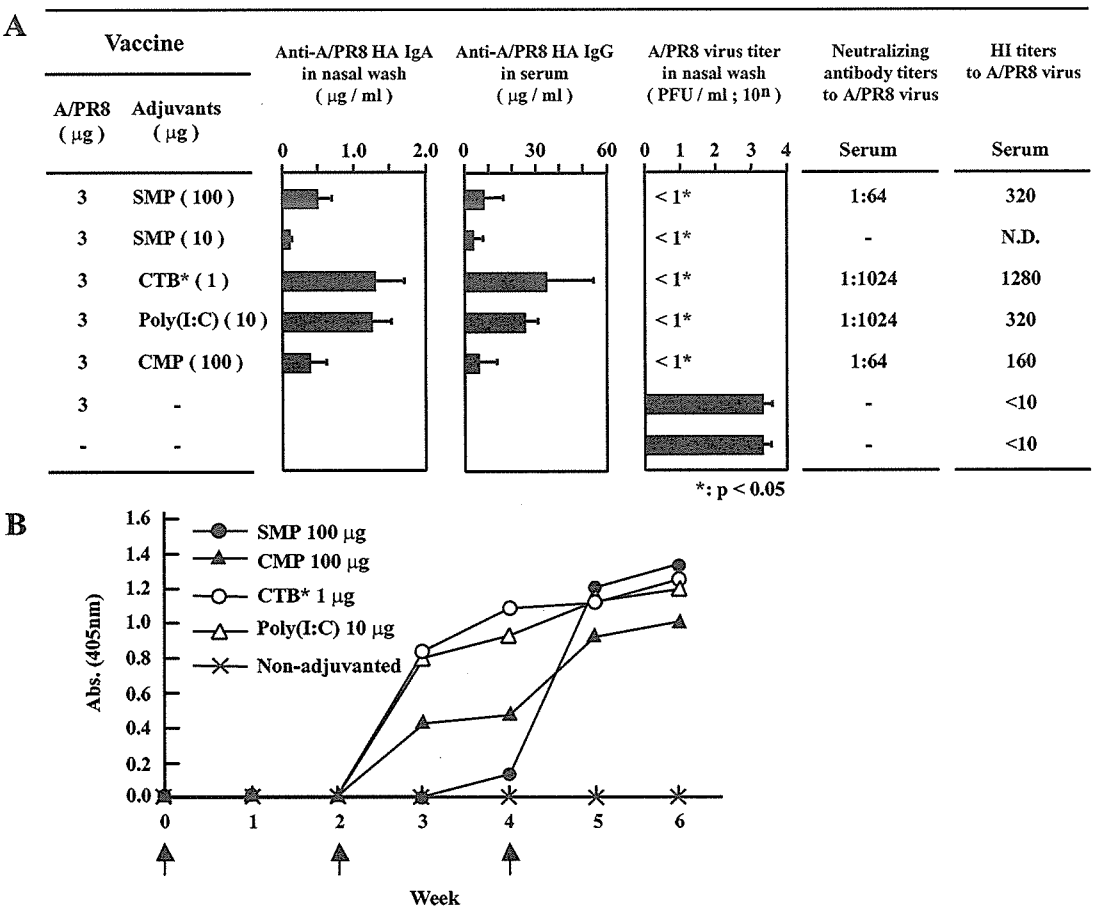

Fig. 1. **A**: Anti-PR8 HA-specific antibody titer and PR8 virus titer. The mice were initially immunized by intranasal administration of 3 μg of HA vaccines with adjuvants, including SMP (100 or 10 μg), CTB*, poly(I:C), or Chitin microparticles (CMP). Immunization was repeated at 3 and 5 weeks after the initial immunization. Two weeks after the final immunization, the mice were challenged by intranasal administration of 1,000 PFU of A/PR8 influenza virus. The nasal wash and serum were collected 3 days after virus challenge. The concentrations of Abs and virus titers of five mice from each group were measured by ELISA and plaque assay using MDCK cells, respectively. Bars represent the means ± S.D. of 5 mice per group. The virus titers were statistically compared to those of non-immunized mice. The neutralizing antibody and HI titers against homologous A/PR8 influenza virus in the serum were measured at 2 weeks after the final immunization. The data are presented per group, where the ability to inhibit 50% of infection at the indicated dilution is shown. HI titers are expressed as reciprocals of the highest dilution that completely inhibits hemagglutination of 4HA units of the virus. The symbol "–" indicates a lack of reduction of infectivity. N.D., not determined. (**B**), Anti-A/PR8 HA IgG titers raised by intranasal inoculation of HA vaccine with adjuvants, including SMP, CTB*, poly(I:C), or CMP. Immunization was repeated at 2 and 4 weeks after the initial immunization. Sera collected at the indicated times from each group were pooled for determination of specific IgG levels by ELISA. Data are represented as the average of two individual assays. Preimmune sera from mice had no detectable specific IgG.

Next, the neutralization activity to A/PR8 virus was examined in vitro using sera from the same group of mice in which antibodies were examined. The neutralization titers of each group of mice immunized with adjuvanted vaccine seemed to parallel the IgG responses in the serum. However, no neutralizing activity was detected in the sera from non-immunized mice or from those immunized with non-adjuvanted vaccine (Fig. 1A). The sera from the same groups of mice were tested for haemagglutination inhibition titers (HI) to A/PR8 virus. The sera of mice immunized with SMP showed HI activity with a titer of 320, which was the same as the titer in mice vaccinated with poly(I:C). No HI titer was detected in the sera from non-immunized mice or from those immunized with non-adjuvanted vaccine (Fig. 1A). Sequential seroconversion of mice immunized intranasally with vaccine with each adjuvant was examined. The serum was collected sequentially from the mice after the first immunization. Final anti-HA IgG titers at 2 weeks after the third immunization were similar in the groups immunized with vaccine with CTB*, poly(I:C), or SMP. However, anti-HA IgG titers appeared faster in the group immunized with vaccine with CTB* or poly(I:C) after the second immunization (Fig. 2B). These results suggest that intranasal administration of HA vaccine with SMP as an adjuvant induces specific antibodies and protects mice against influenza virus infection as well as the other adjuvants.

Intranasal Immunization of HA Vaccine With Surf Clam Microparticles Protects Against Lethal Influenza Virus Lung Infection

The effectiveness of SMP-adjuvanted vaccine for protection against influenza virus-induced lethal pneumonia in BALB/c mice challenged by a lethal dose (40 LD_{50}) of A/PR8 virus at 2 weeks after the final immunization was investigated. Mice immunized with 100 μg of SMP-adjuvanted vaccine showed complete protection against lethal lung infection to an extent similar to that achieved with CTB* as an adjuvant (Fig. 2A). Ten micrograms of SMP-adjuvanted vaccine conferred partial protection against lethal lung infection (four of the five mice showed complete protection, Fig. 2A), while control mice immunized with non-adjuvanted vaccine and non-immunized mice suffered from lung infection (Fig. 2A). The HA-specific IgG antibody was the main antibody present in the lung wash (Fig. 2A), suggesting that IgG antibodies play a role in protection against influenza virus infection in the respiratory bronchioles.

The time course of body weight loss and survival rate of the mice in each group after lethal influenza virus challenge were determined (Fig. 2B). There were no significant changes in body weight in mice treated with SMP or CTB*-adjuvanted vaccine, while the control mice treated with non-adjuvanted vaccine and non-immunized mice showed significant weight reduction at

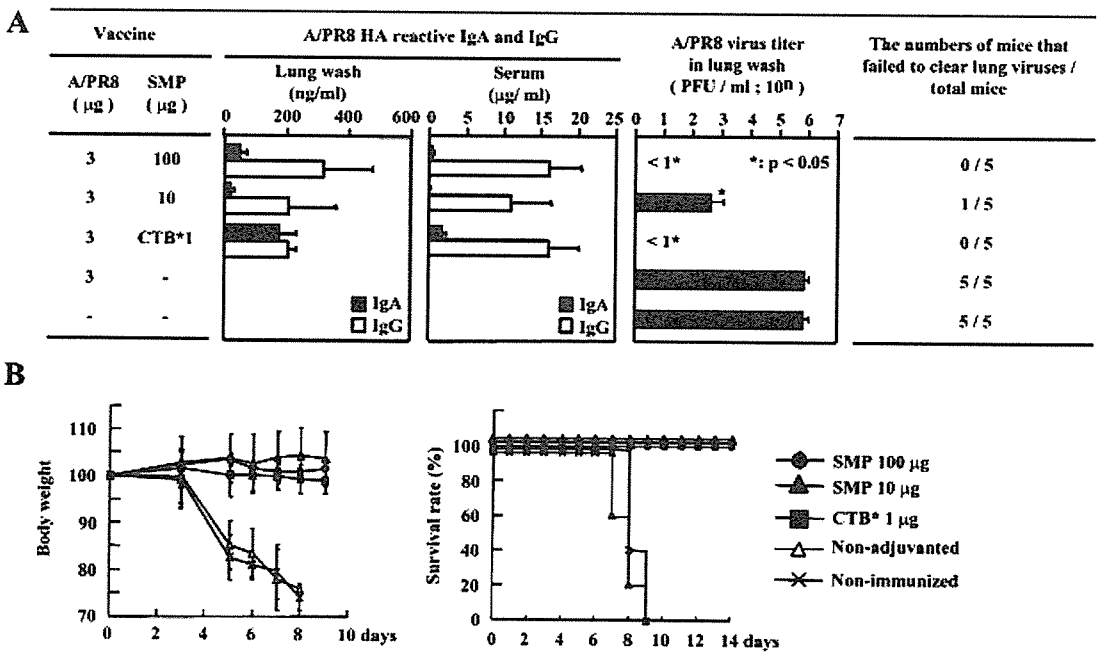

Fig. 2. (**A**), Anti-A/PR8 antibodies in the lung wash and serum, and A/PR8 virus titer in the lung wash. The mice were immunized intranasally with 3 μg of HA vaccines with or without adjuvant (SMP or CTB*) three times. Two weeks after the final immunization, the immunized mice were challenged by administration of 1,000 PFU of A/PR8 influenza virus into the lung, and samples were collected 3 days after the challenge. The concentrations of Abs and virus titers of five mice from each group were measured by ELISA and plaque assay using MDCK cells, respectively. The values shown on the right of the bar graph are numbers of mice that failed to eliminate lung viruses/total mice. Each column represents the mean ± SD of five mice per group. The virus titers were statistically compared to those of non-immunized mice. **B**: The time course of changes in body weight and survival curves of the immunized mice after lethal A/PR8 virus challenge. Each point represents the ratio relative to the initial body weight (mean ± SD) of five mice for each day after challenge (left panel). The survival rates were monitored for 14 days (right panel).

5 days after lethal virus challenge (Fig. 2B). None of the mice survived for more than 9 days after lethal lung infection in the groups treated with non-adjuvanted vaccine and non-immunized mice. In contrast, all mice immunized with SMP-adjuvanted vaccine survived for more than 2 weeks without body weight reduction similar to the group vaccinated with CTB* as an adjuvant (Fig. 2B). These results suggested that intranasal vaccination with SMP adjuvant provides complete protection against lethal influenza pneumonia.

Cross-Protective Effect of Influenza HA Vaccine With Surf Clam Microparticles

Cross-protective effects of SMP-adjuvanted vaccine against various influenza virus subtypes in both nasal-restricted infection and lethal lung infection models were characterized further. The mice were given intranasal immunization three times with various vaccines prepared from A/PR8 (H1N1), A/Yamagata (H1N1), A/Beijing (H1N1), A/Guizhou (H3N2), and B/Ibaraki viruses with SMP as an adjuvant. Two weeks after the final immunization, the immunized mice were challenged intranasally with mouse-adapted A/PR8 virus. Thereafter, the nasal wash virus titer was determined in the nasal-restricted infection model, and the body weight of each mouse was monitored in the lethal lung infection model. A/PR8 was cross-reactive with anti-A/PR8 IgA Abs and the virus titer in the nasal wash and anti-A/PR8 IgG Abs in the serum of the mice immunized with several different influenza strains and SMP (Fig. 3A). The mice immunized with PR8 (H1N1) vaccine showed high-IgA antibody response in the nasal wash, IgG response in the serum, and complete protection against A/PR8 virus infection (Fig. 3A). The mice immunized with A/Yamagata (H1N1), A/Beijing (H1N1), and A/Guizhou (H3N2) also showed cross-reactivity with secreted nasal wash IgA and serum IgG Abs, resulting in prevention of infection with the heterologous virus (A/PR8) (Fig. 3A).

Next, the neutralization activity to A/PR8 virus was examined in vitro using the sera from the same group of mice. The mice immunized with A/PR8 (H1N1) vaccine had neutralized antibodies against A/PR8 (1:64). However, no neutralizing activity was detected in the sera from mice vaccinated with A/Yamagata (H1N1), A/Beijing (H1N1), A/Guizhou (H3N2), or B/Ibaraki influenza virus (Fig. 3A).

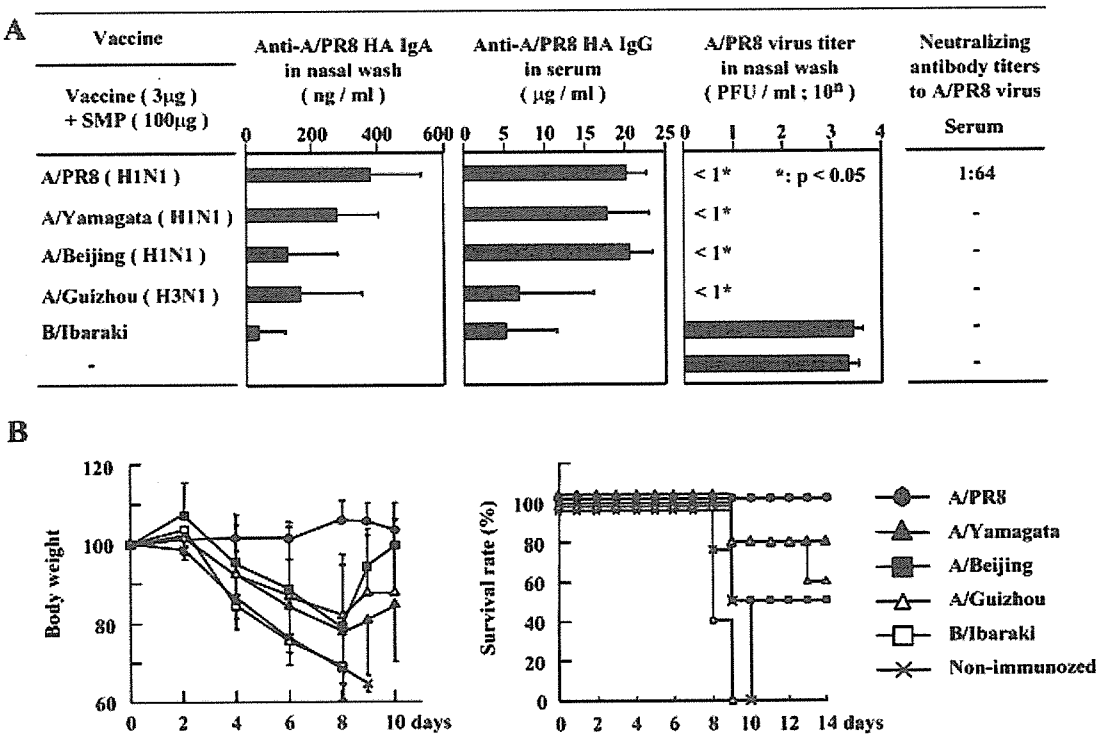

Fig. 3. A: Cross-protective antibody responses against A/PR8 (H1N1) HA in mice immunized intranasally with A/PR8 (H1N1), A/Yamagata (H1N1), A/Beijing (H1N1), A/Guizhou (H3N2), and B/Ibaraki vaccine with 100 μg of SMP three times. Two weeks after the final immunization, the immunized mice were challenged with 1,000 PFU of A/PR8 influenza virus. The nasal wash and serum were collected 3 days after virus challenge. The concentrations of Abs and virus titers of five mice from each group were measured by ELISA and plaque assay using MDCK cells, respectively. Each bar represents the mean ± SD of five mice per group. The virus titers were statistically compared to those of non-immunized mice. The serum collected at 2 weeks after the final immunization was analyzed for the presence of neutralizing antibodies against heterologous A/PR8 influenza virus. The symbol "–" indicates a lack of reduction of infectivity. **B**: The time course of changes in body weight and survival curves of mice immunized according to the same schedule as in (A) after lethal A/PR8 virus challenge. Each point represents the ratio relative to the initial body weight (mean ± SD) of five mice for each day after challenge (left panel). The survival rates were monitored for 14 days (right panel).

To examine the cross-protective effects of SMP-adjuvanted vaccine against lethal influenza virus challenge, mice immunized with vaccines prepared from various strains, including A/PR8 (H1N1), A/Yamagata (H1N1), A/Beijing (H1N1), A/Guizhou (H3N2), and B/Ibaraki, were challenged with a lethal dose (40 LD_{50}) of A/PR8 (H1N1) virus. The body weights of the mice immunized with A/PR8 showed no changes (Fig. 3B). In mice immunized with A/Yamagata, A/Beijing, and A/Guizhou, the body weights decreased gradually until day 8 after challenge, but surviving mice recovered on days 9 and 10 (Fig. 3B). Mice immunized with B/Ibaraki and non-immunized mice showed gradual body weight loss from 2 days after virus challenge (Fig. 3B). All mice immunized with SMP combined with A/PR8 (H1N1) vaccine survived, while the survival rates of mice immunized with SMP combined with A/Yamagata (H1N1), A/Beijing (H1N1), and A/Guizhou (H3N2) ranged from 80% to 50% on day 14 after challenge (Fig. 3B). None of the mice survived in the groups of B/Ibaraki vaccine-immunized or non-immunized mice by 10 days after challenge (Fig. 3B). These observations indicated that intranasal vaccination with SMP adjuvant induces cross-protective immune responses against homologous or heterologous virus infection in the upper and lower respiratory tract.

Intranasal Immunization of HA Vaccine With Surf Clam Microparticles Induces Systemic T-Cell Responses

To examine whether intranasally administered influenza vaccine induces T-cell responses against homologous or heterologous influenza viruses, mice were immunized with several strains of influenza virus, including A/PR8 (H1N1), A/Yamagata (H1N1), A/Beijing (H1N1), A/Guizhou (H3N2), and B/Ibaraki with different adjuvants [SMP, CTB*, poly(I:C), or CMP]. T-cells collected from the spleens of these mice 7 days after the final immunization were enriched and cultured with irradiated APC in the presence or absence of A/PR8 vaccine at 0.1 or 1 μg/ml. The highest level of T-cell proliferation was observed in mice treated with CTB*-adjuvanted vaccine as well as poly(I:C)-adjuvanted vaccine in an antigen dose-dependent manner (Fig. 4A). The mice immunized with SMP-adjuvanted vaccine developed low levels of T-cell proliferation similar to the observations in those immunized with CMP-adjuvanted vaccine (Fig. 4A). T-cells from mice immunized with A/Yamagata and A/Beijing viruses also proliferated. However, no T-cell proliferative effect was observed in mice vaccinated with A/Guizhou or B/Ibaraki virus (Fig. 4A).

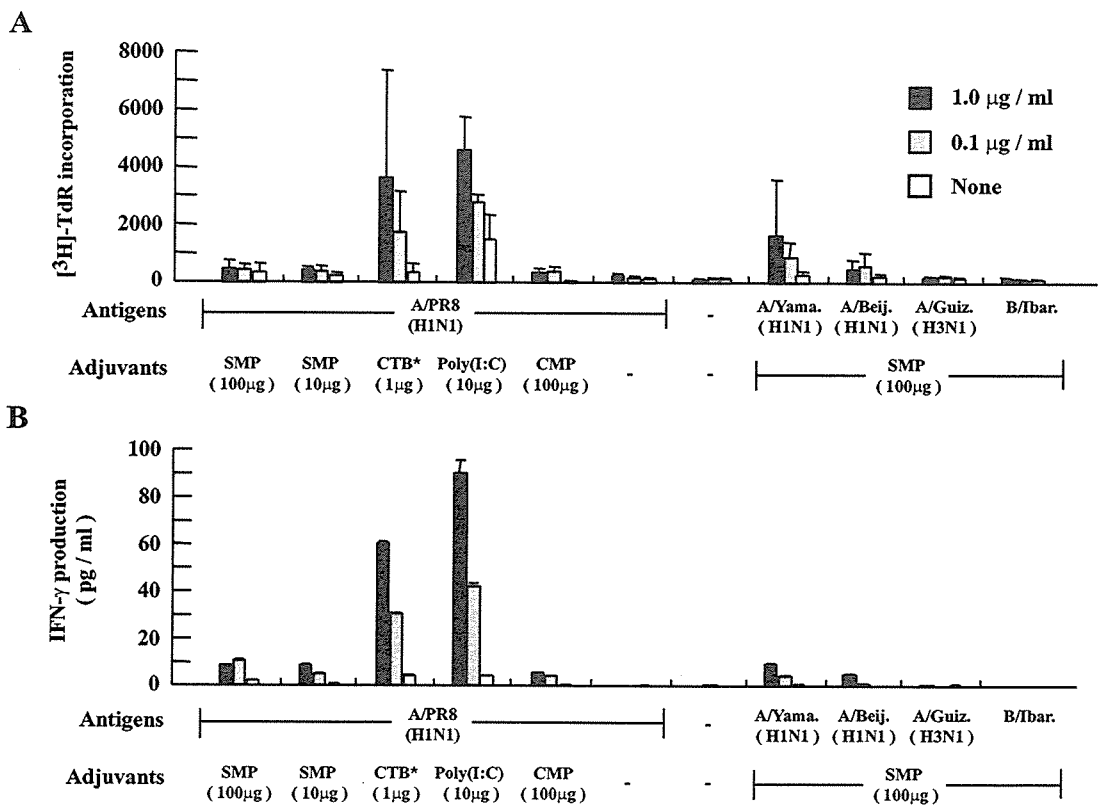

Fig. 4. **A**: In vitro responses of A/PR8 (H1N1) influenza virus-specific T-cells derived from mice vaccinated with A/PR8 (H1N1), A/Yamagata (H1N1), A/Beijing (H1N1), A/Guizhou (H3N2), or B/Ibaraki viruses. The mice were intranasally administered 3 μg of each vaccine with various adjuvants [SMP, CTB*, poly(I:C), or CMP] three times. Spleens were isolated 1 week after the final immunization and stimulated with T-cell-depleted splenocytes that had been pulsed with the indicated concentration of vaccine. These cells were cultured for 4 days and [^{3}H] thymidine was added 8 hr prior to harvest. The [^{3}H] thymidine incorporation is shown in bar graphs. **B**: Production of IFN-γ in the culture supernatant of cells prepared in the same manner as in (A). These results are presented as the means of two independent experiments.

Next, the supernatants of cultured T-cells derived from the spleens of mice immunized under the same conditions as those presented in Figure 4A were examined (Fig. 4B). IFN-γ levels were relatively high in the supernatants of cultured T-cells from mice vaccinated with CTB* and poly(I:C), while IFN-γ levels were low in those from mice vaccinated with SMP and CMP (Fig. 4B).

IFN-γ production was detected in T-cells from mice treated with A/Yamagata and A/Beijing but not in those immunized with A/Guizhou (H3N2) or B/Ibaraki (Fig. 4B). Thus, IFN-γ production seemed to parallel T-cell proliferation in mice immunized with adjuvanted vaccines. These results suggested that T-cell responses against heterologous influenza viruses were relatively weak.

Safety of Intracerebral, Intraperitoneal, Intranasal, and Intragastric Injection of Surf Clam Microparticles

The safety of SMP was examined by intracerebral (i.c.), intraperitoneal (i.p.), intranasal (i.n.), and intragastric (i.g.) administration of an excess of particles into mice. The i.c. and i.p. groups received a single administration of 250 μg or 1 mg of SMP, respectively, while the i.n. and i.g. groups received a daily dose of 100 μg or 1 mg of the adjuvant, respectively. There were no significant changes in body weight of mice in any of the groups treated with SMP as compared with the negative control group (Fig. 5A).

Histopathological examination revealed no pathological changes in the nasal area of mice treated i.n. with SMP daily for 23 days or in controls treated with PBS alone (Fig. 5B,C). As the nasal cavity is connected anatomically to the brain via the olfactory nerves, the effects of intracerebral administration of SMP were examined. Inflammatory cells were recognized in the area surrounding the injection sites (somatosensory barrel field) of mice administered SMP or PBS, and no differences were observed between the two groups (data not shown). In addition, no pathological changes were observed in the heart, lung, stomach, spleen, liver, or kidney in the i.p. or i.g. administration groups or in the control group. These results suggested that intracerebral, intraperitoneal, intranasal, and intragastric injection of SMP are not harmful to the mice.

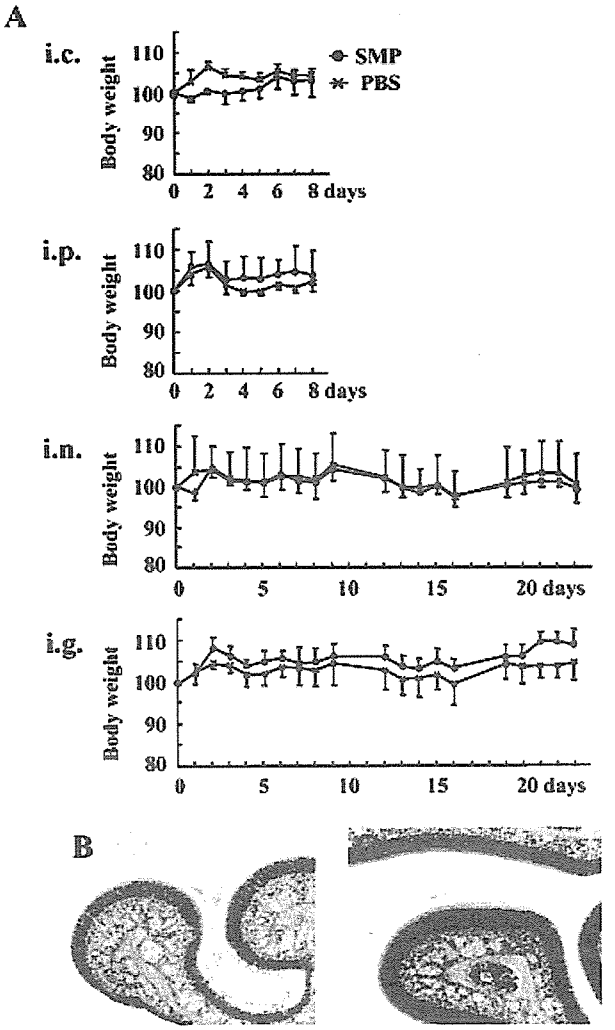

Fig. 5. **A**: The time course of changes in body weight of immunized mice after a single intracerebral (i.c.) or intraperitoneal (i.p.) infection of 250 μg or 1 mg of surf clam microparticles (SMP), respectively. Intranasal (i.n.) and intragastric (i.g.) administration were performed daily for 23 days with 100 μg or 1 mg of SMP, respectively. Each point represents the ratio relative to the initial body weight (mean ± SD%) of 5 mice on each day. **B, C**: Histopathological finding of the nasal cavity of mice administered 100 μg of SMP (B) or PBS (C) intranasally daily for 23 days (×100, H&E staining).

DISCUSSION

The results of the present study clearly demonstrated that SMP is an effective mucosal adjuvant when administered intranasally with influenza vaccine. It has been reported that effective immunization strategies to protect against influenza virus infection involve the induction of mucosal immune responses at the nasal mucosal epithelium, which is the initial target of virus infection [Tamura et al., 1989a; Hasegawa et al., 2000]. For effective protection against influenza virus infection at the mucosa, bacterial toxin-derived adjuvants, such as CT or LT, have been administered in conjunction with immunization [Tamura et al., 1988, 1989a,b, 1994; Komase et al., 1998; Hagiwara et al., 1999]. To reduce the toxicity of bacterial toxin-derived adjuvants, mutant toxins [Hagiwara et al., 1999, 2001] or low doses of CTB subunits with trace amounts (0.1%) of holotoxin (CTB*) [Tamura et al., 1995] have been applied in experimental animal models. However, application of these adjuvants to human vaccination strategies is still somewhat problematic [van Ginkel et al., 2000], and there is still a need for an effective and safe adjuvant for intranasal vaccination that is applicable to humans. This report presented a new adjuvant system for intranasal vaccination without bacterial toxins or derivatives.

A major objective of intranasal influenza vaccine development is the design of an adjuvant that can provide both effective immune activity and is safe for

clinical application in humans. Surf clam microparticles is an adjuvant derived from a natural non-microbial source that induces anti-HA antibodies when administered intranasally with vaccine using the three-dose immunization protocol. Nasal immunization evoked not only an increase in mucosal secretory IgA, but also a high titer of anti-HA IgG in the serum. This immune response resulted in protection against influenza viral challenge, including both the upper respiratory tract-restricted influenza model and the lung infection pneumonia model. The PR8 HA vaccine combined with 100 μg of SMP in the three-dose immunization protocol conferred complete protection against lethal lung infection (40 LD_{50}) by PR8 influenza virus. These results indicate that SMP is an effective mucosal adjuvant when administered intranasally with influenza vaccine.

The nasal route of vaccination is advantageous for protection against influenza virus infection due to the induction of secretory IgA in the mucosal epithelium, which elicits more effective cross-protective immunity as compared with serum IgG [Tamura et al., 1992]. In fact, cross-protective effects of the SMP-adjuvanted vaccine were observed. In the present study, HA vaccines from various strains of influenza virus, including A/PR8 (H1N1), A/Yamagata (H1N1), A/Beijing (H1N1), A/Guizhou (H3N2), and B/Ibaraki, with 100 μg of SMP in the three-dose immunization protocol were used. Among these vaccines, PR8-HA-reactive secretory IgA and IgG were detected in the nasal wash and serum, respectively, in mice immunized with variant viruses. However, the neutralizing activity of the serum against A/PR8 virus was observed exclusively in mice immunized with homologous virus. No neutralizing activity was detected in the nasal wash in any group in the present study. The concentration of anti-A/PR8 HA IgA in the nasal wash was much lower than that of anti-A/PR8 HA IgG in the serum, because the nasal wash was diluted with PBS for collection from the nasal mucosa. It seems that the concentration of anti-A/PR8 HA IgA is much lower than the physiological concentration in the nasal mucosa, and therefore neutralizing activity in the nasal wash may not be detected. Mice that had IgA to cross-reactive A/PR8 virus in the nasal wash fluid were protected against lethal viral challenge. Antigen-specific T-cell responses and weak cross-reactivity in mice treated with heterologous viruses were observed. These mice showed protection against viral challenge, although mice immunized with the B/Ibaraki strain influenza vaccine failed to eliminate the A/PR8 influenza virus. Thus, homologous and heterologous protection may be accomplished by cross-reactive s-IgA, although other mechanisms may also be involved. The mechanism of the adjuvant effect of SMP is still unclear. However, SMP, which consists of microparticles 1–10 μm in diameter, may act as carrier for phagocytosis by macrophages and dendritic cells. Phagocytosis of a protein antigen in particle-adsorbed form (1 μm polystyrene particles), as compared with the soluble form, by progenitor dendritic cells was reported to involve an activation event [Scheicher et al., 1995].

Prophylactic agents, including vaccines, should have sufficient safety for clinical use. As the nasal cavity and the forebrain communicate directly via the olfactory nerve, the safety of nasal administration of the vaccine with adjuvant for the central nervous system should be confirmed. The safety of SMP in the central nervous system was demonstrated by direct intracerebral injection. Moreover, the use of an inactivated vaccine with safe adjuvant and not a living virus is very important with regard to safety, because influenza vaccine is recommended for high-risk populations, such as infants and the elderly. Therefore, SMP adjuvant is a good candidate as a new, effective, and safe mucosal adjuvant when administered intranasally with influenza vaccine for use in humans. Further studies are required to determine whether such a nasal vaccine would be effective in humans.

ACKNOWLEDGMENTS

We are grateful to Mr. Y. Yamaguchi (Daido Sangyo Co., Ltd., Tokyo, Japan) for providing the materials, Dr. A. Ninomiya and Dr. W.W. Hall for helpful discussion and Ms. A. Harashima for technical assistance. This work was supported in part by grants from the Ministry of Health, Labour and Welfare and Research on Health Sciences focusing on Drug Innovation.

REFERENCES

Asahi Y, Yoshikawa T, Watanabe I, Iwasaki T, Hasegawa H, Sato Y, Shimada S, Nanno M, Matsuoka Y, Ohwaki M, Iwakura Y, Suzuki Y, Aizawa C, Sata T, Kurata T, Tamura S. 2002. Protection against influenza virus infection in polymeric Ig receptor knockout mice immunized intranasally with adjuvant-combined vaccines. J Immunol 168:2930–2938.

Coulter A, Harris R, Davis R, Drane D, Cox J, Ryan D, Sutton P, Rockman S, Pearse M. 2003. Intranasal vaccination with ISCOMATRIX adjuvanted influenza vaccine. Vaccine 21:946–949.

Davenport FM, Hennessy AV, Brandon FM, Webster RG, Barrett CD, Jr., Lease GO. 1964. Comparisons of serologic and febrile responses in humans to vaccination with influenza a viruses or their hemagglutinins. J Lab Clin Med 63:5–13.

Hagiwara Y, Komase K, Chen Z, Matsuo K, Suzuki Y, Aizawa C, Kurata T, Tamura S. 1999. Mutants of cholera toxin as an effective and safe adjuvant for nasal influenza vaccine. Vaccine 17:2918–2926.

Hagiwara Y, Iwasaki T, Asanuma H, Sato Y, Sata T, Aizawa C, Kurata T, Tamura S. 2001. Effects of intranasal administration of cholera toxin (or *Escherichia coli* heat-labile enterotoxin) B subunits supplemented with a trace amount of the holotoxin on the brain. Vaccine 19:1652–1660.

Hasegawa H, Kadowaki S, Takahashi H, Iwasaki T, Tamura S, Kurata T. 2000. Protection against influenza virus infection by nasal vaccination in advance of sublethal irradiation. Vaccine 18:2560–2565.

Hasegawa H, Ichinohe T, Strong P, Watanabe I, Ito S, Tamura S, Takahashi H, Sawa H, Chiba J, Kurata T, Sata T. 2005. Protection against influenza virus infection by intranasal administration of hemagglutinin vaccine with chitin microparticles as an adjuvant. J Med Virol 75:130–136.

Ichinohe T, Watanabe I, Ito S, Fujii H, Moriyama M, Tamura S, Takahashi H, Sawa H, Chiba J, Kurata T, Sata T, Hasegawa H. 2005. Synthetic double-stranded RNA poly(I:C) combined with mucosal vaccine protects against influenza virus infection. J Virol 79:2910–2919.

Jackson LA, Holmes SJ, Mendelman PM, Huggins L, Cho I, Rhorer J. 1999. Safety of a trivalent live attenuated intranasal influenza vaccine, FluMist, administered in addition to parenteral trivalent inactivated influenza vaccine to seniors with chronic medical conditions. Vaccine 17:1905–1909.

Komase K, Tamura S, Matsuo K, Watanabe K, Hattori N, Odaka A, Suzuki Y, Kurata T, Aizawa C. 1998. Mutants of *Escherichia coli* heat-labile enterotoxin as an adjuvant for nasal influenza vaccine. Vaccine 16:248–254.

Mutsch M, Zhou W, Rhodes P, Bopp M, Chen RT, Linder T, Spyr C, Steffen R. 2004. Use of the inactivated intranasal influenza vaccine and the risk of Bell's palsy in Switzerland. N Engl J Med 350:896–903.

Phelan MA, Mayner RE, Bucher DJ, Ennis FA. 1980. Purification of influenza virus glycoproteins for the preparation and standardization of immunological potency testing reagents. J Biol Stand 8:233–242.

Piedra PA, Yan L, Kotloff K, Zangwill K, Bernstein DI, King J, Treanor J, Munoz F, Wolff M, Cho I, Mendelman PM, Cordova J, Belshe RB. 2002. Safety of the trivalent, cold-adapted influenza vaccine in preschool-aged children. Pediatrics 110:662–672.

Scheicher C, Mehlig M, Dienes HP, Reske K. 1995. Uptake of microparticle-adsorbed protein antigen by bone marrow-derived dendritic cells results in up-regulation of interleukin-1 alpha and interleukin-12 p40/p35 and triggers prolonged, efficient antigen presentation. Eur J Immunol 25:1566–1572.

Sever JL. 1962. Application of a microtechnique to viral serological investigations. J Immunol 88:320–329.

Smidt MH, Stroink H, Bruinenberg JF, Peeters M. 2004. Encephalopathy associated with influenza A. Eur J Paediatr Neurol 8:257–260.

Takasuka N, Fujii H, Takahashi Y, Kasai M, Morikawa S, Itamura S, Ishii K, Sakaguchi M, Ohnishi K, Ohshima M, Hashimoto S, Odagiri T, Tashiro M, Yoshikura H, Takemori T, Tsunetsugu-Yokota Y. 2004. A subcutaneously injected UV-inactivated SARS coronavirus vaccine elicits systemic humoral immunity in mice. Int Immunol 16:1423–1430.

Tamura S, Kurata T. 1997. Mucosal immune responses against influenza virus. Nippon Rinsho 55:2725–2731.

Tamura SI, Kurata T. 2000. A proposal for safety standards for human use of cholera toxin (or *Escherichia coli* heat-labile enterotoxin) derivatives as an adjuvant of nasal inactivated influenza vaccine. Jpn J Infect Dis 53:98–106.

Tamura S, Samegai Y, Kurata H, Nagamine T, Aizawa C, Kurata T. 1988. Protection against influenza virus infection by vaccine inoculated intranasally with cholera toxin B subunit. Vaccine 6:409–413.

Tamura S, Kurata H, Funato H, Nagamine T, Aizawa C, Kurata T. 1989a. Protection against influenza virus infection by a two-dose regimen of nasal vaccination using vaccines combined with cholera toxin B subunit. Vaccine 7:314–320.

Tamura SI, Samegai Y, Kurata H, Kikuta K, Nagamine T, Aizawa C, Kurata T. 1989b. Enhancement of protective antibody responses by cholera toxin B subunit inoculated intranasally with influenza vaccine. Vaccine 7:257–262.

Tamura S, Ito Y, Asanuma H, Hirabayashi Y, Suzuki Y, Nagamine T, Aizawa C, Kurata T. 1992. Cross-protection against influenza virus infection afforded by trivalent inactivated vaccines inoculated intranasally with cholera toxin B subunit. J Immunol 149:981–988.

Tamura S, Asanuma H, Tomita T, Komase K, Kawahara K, Danbara H, Hattori N, Watanabe K, Suzuki Y, Nagamine T, et al. 1994. Escherichia coli heat-labile enterotoxin B subunits supplemented with a trace amount of the holotoxin as an adjuvant for nasal influenza vaccine. Vaccine 12:1083–1089.

Tamura S, Ishihara K, Miyata K, Aizawa C, Kurata T. 1995. Mechanism of enhancement of the immune responses to influenza vaccine with cholera toxin B subunit and a trace amount of holotoxin. Vaccine 13:339–341.

Tamura S, Miyata K, Matsuo K, Asanuma H, Takahashi H, Nakajima K, Suzuki Y, Aizawa C, Kurata T. 1996. Acceleration of influenza virus clearance by Th1 cells in the nasal site of mice immunized intranasally with adjuvant-combined recombinant nucleoprotein. J Immunol 156:3892–3900.

Tamura S, Iwasaki T, Thompson AH, Asanuma H, Chen Z, Suzuki Y, Aizawa C, Kurata T. 1998. Antibody-forming cells in the nasal-associated lymphoid tissue during primary influenza virus infection. J Gen Virol 79:291–299.

Tobita K. 1975. Permanent canine kidney (MDCK) cells for isolation and plaque assay of influenza B viruses. Med Microbiol Immunol (Berl) 162:23–27.

Tobita K, Sugiura A, Enomote C, Furuyama M. 1975. Plaque assay and primary isolation of influenza A viruses in an established line of canine kidney cells (MDCK) in the presence of trypsin. Med Microbiol Immunol (Berl) 162:9–14.

van Ginkel FW, Jackson RJ, Yuki Y, McGhee JR. 2000. Cutting edge: The mucosal adjuvant cholera toxin redirects vaccine proteins into olfactory tissues. J Immunol 165:4778–4782.

Wada N. 2004. Influenza-associated encephalopathy. Nippon Rinsho 62:456–461.

Watanabe I, Hagiwara Y, Kadowaki SE, Yoshikawa T, Komase K, Aizawa C, Kiyono H, Takeda Y, McGhee JR, Chiba J, Sata T, Kurata T, Tamura S. 2002. Characterization of protective immune responses induced by nasal influenza vaccine containing mutant cholera toxin as a safe adjuvant (CT112K). Vaccine 20:3443–3455.

Watanabe I, Ross TM, Tamura S, Ichinohe T, Ito S, Takahashi H, Sawa H, Chiba J, Kurata T, Sata T, Hasegawa H. 2003. Protection against influenza virus infection by intranasal administration of C3d-fused hemagglutinin. Vaccine 21:4532–4538.

Yetter RA, Lehrer S, Ramphal R, Small PA, Jr. 1980. Outcome of influenza infection: Effect of site of initial infection and heterotypic immunity. Infect Immun 29:654–662.

Available online at www.sciencedirect.com
ScienceDirect
Microbes and Infection 8 (2006) 2706–2714
Microbes and Infection
www.elsevier.com/locate/micinf

Original article

Intranasal administration of adjuvant-combined recombinant influenza virus HA vaccine protects mice from the lethal H5N1 virus infection

Yasuko Asahi-Ozaki [a], Shigeyuki Itamura [b], Takeshi Ichinohe [a,1], Peter Strong [c], Shin-ichi Tamura [a], Hidehiro Takahashi [a], Hirofumi Sawa [d], Masami Moriyama [e], Masato Tashiro [b], Tetsutaro Sata [a], Takeshi Kurata [a], Hideki Hasegawa [a,*]

[a] *Department of Pathology, National Institute of Infectious Diseases, 4-7-1 Gakuen, Musashimurayama-shi, Tokyo 208-0011, Japan*
[b] *Department of Virology III, National Institute of Infectious Diseases, Tokyo, Japan*
[c] *Medical Research Council Immunochemistry Unit, University of Oxford, Oxford, UK*
[d] *Department of Molecular Pathobiology, and 21st Century COE Program for Zoonosis Control, Hokkaido University Research Center for Zoonosis Control, N15, W7, Kita-ku, Sapporo 060-8638, Japan*
[e] *Department of Microbiology and Immunology, School of Medicine, Keio University, 35 Shinano-machi, Shinjyuku-ku, Tokyo 160-8582, Japan*

Received 1 June 2006; accepted 30 July 2006
Available online 28 August 2006

Abstract

Attenuated recombinant H5N1 influenza virus was constructed to develop a safe H5N1 influenza vaccine. The immunogenicity and protective effect of the vaccine prepared from haemagglutinin-modified recombinant H5N1 influenza virus was evaluated in mice intranasally co-administered with cholera toxin B subunit containing a trace amount of holotoxin (CTB*), synthetic double-stranded RNA, poly (I:C) or chitin microparticles (CMP) as adjuvants. Intranasal administration of recombinant H5 HA split vaccine with CTB* or poly(I:C) and/or CMP elicited an immunological response with both anti-H5 HA IgA in the nasal wash and anti-H5 HA IgG antibody in the serum, and showed a protective against lethal H5N1 A/Hong Kong/483/97 (HK483) infection. We also demonstrated that intranasal co-administration of antigen with both poly (I:C) and CMP enhanced the expression of Toll-like receptor (TLR) 3, TLR7 in the spleen. These results indicate that poly (I:C) and CMP are highly effective as mucosal adjuvants for use with the nasal H5N1 vaccine.

Keywords: H5N1; Double-stranded RNA (dsRNA); Poly (I:C); Chitin microparticle (CMP); Adjuvant; IgA; Toll-like receptor (TLR)

1. Introduction

In 1997, the highly pathogenic avian influenza A virus strain, H5N1, transmitted directly from chickens to humans killed 6 of 18 infected people in Hong Kong [1,2]. In 2003–2005, the H5N1 virus caused outbreaks in poultry in East Asian countries, and again transmission of infection from birds to humans resulted in fatal disease [3]. The development of an anti-H5N1 vaccine is the best strategy to prevent a potential human pandemic of this virus. However, it was not possible to prepare a vaccine against the Hong Kong H5N1 virus using the conventional embryonated egg system because of its lethality in chicken embryos [4]. Avirulent recombinant H5N1/PR8 virus for use as a vaccine was established using a reverse genetics technique [5]. We have also established an avirulent recombinant H5N1 virus strain with a genetically modified haemagglutinin (HA) derived from the human

* Corresponding author. Tel.: +81 42 561 0771; fax: +81 42 561 6572.
E-mail address: hasegawa@nih.go.jp (H. Hasegawa).
[1] Research Fellow of the Japan Society for the Promotion of Science.

1286-4579/$ - see front matter © 2006 Elsevier Masson SAS. All rights reserved.
doi:10.1016/j.micinf.2006.07.018

H5N1 virus genome (Itamura & Nishimura, unpublished data), and a split-product virus vaccine was prepared using this HA-modified virus by conventional procedures [6].

Following subcutaneous administration, the inactivated vaccines induce systemic anti-viral IgG antibodies (Abs) that are highly protective against homologous virus infection but are less effective against heterologous drifted virus infection [7]. However, many studies have shown that secretory IgA (S-IgA) induced by natural infection is more cross-protective against viral infection than serum IgG induced by parenteral vaccines in humans and mice [8]. In addition, S-IgA is primarily involved in protection against infection in the upper respiratory tract, whereas serum IgG plays a role in the lower respiratory tract [9].

Previously, we demonstrated that intranasal immunisation of mice with a mixture of inactivated A or B influenza virus vaccine and cholera toxin B subunits containing a trace amount of the holotoxin (CTB*) induced both S-IgA and serum IgG [10]. We also found that S-IgA plays an important role in cross-protection against variant A and B virus infection [11,12]. In this regard, induction of S-IgA in the upper respiratory tract shows marked advantages in protection against unpredictable epidemics of influenza. Although CTB* is an effective adjuvant to produce S-IgA, it has clinical side effects, such as nasal discharge. The use of *Escherichia coli* heat-labile enterotoxin (LT), which is structurally and functionally similar to cholera toxin (CT), as an adjuvant with the nasal influenza vaccines may not be clinically safe, as intranasal influenza vaccine with LT has been linked to several cases of Bell's palsy (facial paralysis) [13]. Therefore, attempts to reduce the toxic side effects have involved the introduction of mutations into CTB [14] or by using physiological adjuvants, such as the complement component, C3d [15]. Clinically safe and more effective adjuvants are necessary for the employment of an intranasal influenza vaccine.

Recently, double-stranded RNA (dsRNA) has been reported to act as a molecular mimic associated with viral infection, because most RNA viruses produce dsRNA during their replication [16]. It has also been shown that mammalian Toll-like receptor (TLR) 3 recognises dsRNA and activates the NF-κB [17] pathway, resulting in activation of type I interferon (IFN-I), which enhances the primary antibody response against subcutaneous immunisation of soluble materials [18]. Single-stranded RNA (ssRNA) derived from influenza virus acts as a ligand for TLR 7 and induces TLR7-dependent production of IFN-α [19]. Previously, we demonstrated that the mucosal adjuvant activity of intranasal administration of synthetic dsRNA, poly (I:C) with inactivated influenza HA vaccine induces cross-protective immune responses against homologous and heterologous variant influenza virus infection [20]. In addition, chitin microparticles (CMP) were applied as an adjuvant to mice with HIV-DNA vaccine, bacterial antigen, or influenza (H1N1) HA vaccine, and resulted in both up-regulation of Th1 cytokine expression and suppression of IL-4 with reduction of allergic symptoms [21,22].

In the present study, we showed that co-administration of vaccine prepared from recombinant avirulent avian influenza virus with both poly (I:C) and CMP as mucosal adjuvants elicits protective immunity against highly pathogenic influenza virus H5N1 infection.

2. Materials and methods

2.1. Preparation of vaccine and adjuvants

A recombinant vaccine strain was produced using reverse genetics techniques. Briefly, the haemagglutinin gene of A/HongKong/156/97 (H5N1) from which the polybasic amino acid motif at the cleavage site PQRERRRKKR/G was changed to PQRETR/G, was introduced into the avirulent avian influenza A/duck/Hong Kong/836/80 (H3N1) virus as a helper strain. Using this virus (HK9-1-1, H5N1), a split-product virus vaccine was prepared in accordance with conventional methods [6,23]. The virus, grown in the allantoic cavities of 10- to 11-day embryonated hen's eggs, was concentrated, highly purified and disrupted with ether. The vaccine contained whole proteins from the virus particles, consisting mainly of HA molecules (~30% of the total protein).

Cholera toxin B subunit containing trace amounts of holotoxin (CTB*) was prepared by adding 0.1% holotoxin to cholera toxin B (Sigma, St. Louis, MO, USA). Synthetic dsRNA [poly (I:C)] was kindly provided by Toray Industries, Inc. (Kamakura, Kanagawa, Japan). CMP were prepared by sonication of dissolved purified chitin (Sigma-Aldrich, Poole, UK) in sterile, endotoxin-free phosphate-buffered saline (PBS) [21].

2.2. Immunisation protocols

All animal experiments were carried out in accordance with the Guides for Animal Experiments Performed at NIID and approved by the International Animal Care and Use Committee of the NIID. Groups of fifteen 7-week-old female BALB/c mice, or fifteen 23-week-old female B10 mice (Japan SLC Inc., Hamamatsu, Japan) were anaesthetised with diethyl ether and received a primary vaccination with 0.1–2 μg of viral protein along with 0.1–100 μg of each adjuvant or vaccine alone in a volume of 1–10 μl into each nostril. Four weeks later, they were re-immunised in the same manner with 2 μg of vaccine alone or with the same adjuvants. Two weeks after the second immunisation, five mice from each group were sacrificed to examine pre-challenge antibody responses and count the number of antibody-forming cells (AFCs), while the remaining mice were challenged intranasally with wild-type H5N1 A/Hong Kong/483/97 (HK483) virus to examine clinical signs, changes in body weight, and survival rate for 18 days.

2.3. Virus infection

HK483 virus isolated from a human patient was subcultured four times in Madin-Darby canine kidney (MDCK) cells. In accordance with a slight modification of the procedure of Yetter and co-workers [24], the mice were anaesthetised

with amobarbital sodium (0.25 ml of a 1 μg/ml solution) two weeks after the second immunisation, and 1 μl of the HK483 virus suspension was introduced into each nostril (2 μl per mouse, 100 LD_{50}). Challenge infection experiments using infectious virus were carried out under biosafety level 3 containment approved by the Guides for Animal Experiments Performed at NIID and the International Animal Care and Use Committee of the NIID.

2.4. Enzyme-linked immunosorbent assay (ELISA) for anti-H5-HA, IgA, and IgG antibodies

For measurement of anti-H5-HA antibodies, pre-challenge serum specimens were obtained from the hearts of anaesthetised mice, and nasal wash specimens were collected by washing with 1 ml of PBS containing 0.1% BSA from the nasal cavity of the excised head [10,11]. The IgA and IgG antibodies levels against recombinant HA protein of A/HongKong/483/97 (H5N1) was purified from baculovirus-infected insect cells (Katakura Industries Co., Ltd., Saitama, Japan) were determined by ELISA as described previously [11]. Standards for H5-HA-reactive IgA or IgG antibody titration were prepared as described previously [11], and expressed as the same arbitrarily units (160-unit). The antibody titres of unknown specimens were determined from the standard regression curve constructed by twofold serial dilution of the 160-unit standard for each assay.

2.5. Enzyme-linked immunospot (ELISPOT) assay

Mice were sacrificed two weeks after the second intranasal immunisation, and NALTs and spleens were removed as described previously [25]. The H5-HA protein-specific AFCs were enumerated by ELISPOT assay as described previously with minor modifications [26].

2.6. RNA isolation, cDNA synthesis, and real-time PCR

Expression of mRNAs of Toll-like receptors (TLR3, TLR4 and TLR7) in nasal-associated lymphoid tissues (NALTs) and spleens of immunised mice was examined by real-time quantitative RT-PCR. NALTs and spleens were collected from mice intranasally administered vaccine with adjuvant sequentially 6, 24, 72 h and 7 days post-immunisation. Total RNA was extracted from the NALTs and spleen of mice using an SV-Total RNA Isolation kit (Promega, Madison, WI, USA), and cDNA was synthesised using oligo-dT primer and the Omniscript Reverse Transcriptase (Qiagen, GmbH, Hilden, Germany) in accordance with the manufacturer's instructions.

Real-time quantitative RT-PCR was performed using an ABI PRISM 7900HT sequence detection system (using Ver.2.1 Software; Applied Biosystems, Foster City, CA, USA) with a QuantiTect Probe PCR kit (Qiagen), TaqMan probes, and primers (Sigma Genosys, Ishikari, Japan) designed with Primer Express (Applied Biosystems) as described previously [20]. Quantitative results were obtained using the standard curves of cycle thresholds generated from pGEM-T plasmid containing each target sequence. All data were calibrated relative to β-actin mRNA level as an endogenous internal control. Samples were considered negative if the copy number was below 10.

2.7. Pathology and immunohistochemistry of the challenged mice

Mice from either the non-immunized group or the immunised group [2 μg of vaccine combined with 10 μg of poly

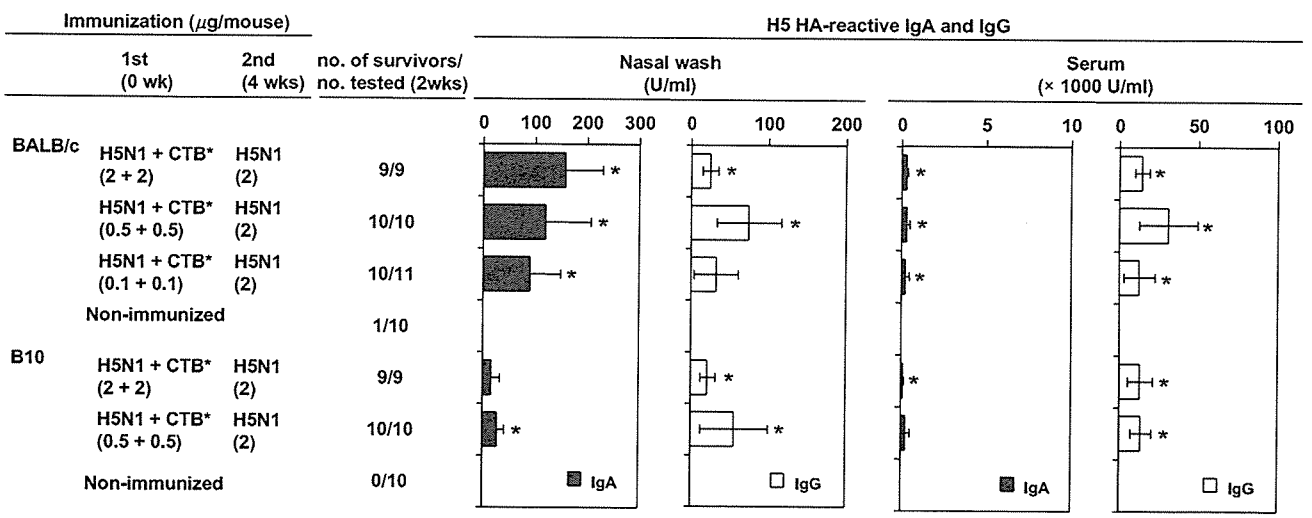

Fig. 1. Anti-H5 HA-specific IgA and IgG responses in BALB/c mice and B10 mice, and their survival rates after lethal challenge with H5N1 virus. Anti-H5 HA-specific IgA and IgG responses in BALB/c mice and B10 mice that received primary intranasal immunisation with 0.1 to 2 μg of H5 vaccine with CTB* as an adjuvant. Secondary immunisation was performed 4 weeks after primary immunisation without adjuvant. Nasal washes and serum samples were collected 2 weeks after the second immunisation. The antibody titres of the nasal wash and serum samples from five mice in each group were measured by ELISA. Mice immunised in the same way ($n = 9–11$) were infected intranasally with 100 LD_{50} of HK483 virus suspension 2 weeks after the second immunisation and their survival rates were observed. Each column represents the mean ± standard deviation (S.D.). The antibody titres were compared statistically with those of non-immunised mice with the t-test for paired observations. *$p < 0.05$.

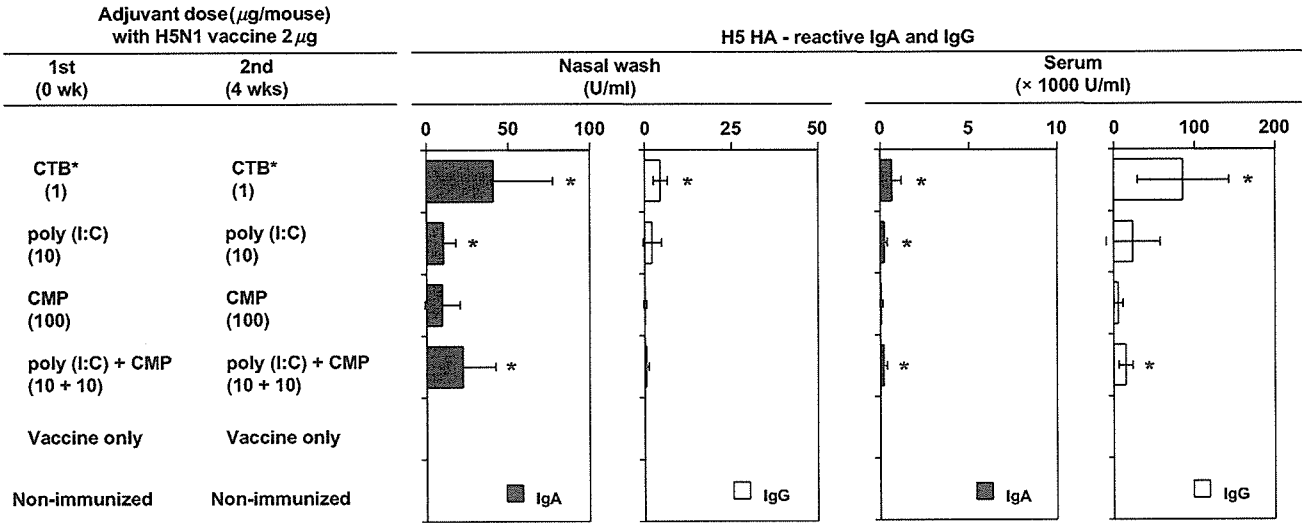

Fig. 2. Anti-H5 HA-specific antibody titre. Anti-H5 HA-specific IgA and IgG responses in BALB/c mice that received primary intranasal immunisation with 2 μg of H5 vaccine with CTB*, poly (I:C), CMP, or poly (I:C) + CMP as an adjuvant. Secondary immunisation was performed 4 weeks after primary immunisation with the same adjuvant. Nasal washes and serum samples were collected 2 weeks after the second immunisation. The antibody titres of five mice from each group were measured by ELISA. Each column represents the mean ± S.D. The antibody titres were compared statistically with those of non-immunised mice with the *t*-test for paired observations. $*p < 0.05$.

(I:C) plus 10 μg CMP] were sacrificed at 7 days post-infection for histopathological analysis. Tissues were fixed in 4% (v/v) of phosphate-buffered formalin. The tissues were then dehydrated and embedded in paraffin. Serial sections were prepared and stained with haematoxylin and eosin (H&E) solution or subjected to immunohistochemical staining with antiserum against the nucleoprotein (NP) of influenza A/PuertoRico/8/34 virus. The specificity of the anti-NP antibody and the reactivity of the antibody to H5N1 influenza virus were confirmed previously [27]. Immunohistochemical staining was performed by the avidin-streptavidin-peroxidase method using 3-3′diaminobenzidine as a substrate.

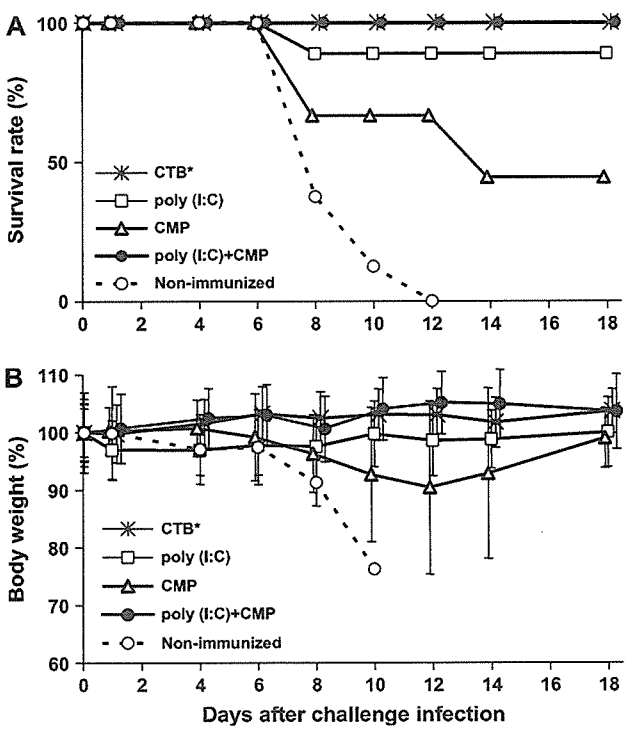

Fig. 3. Survival rates and changes in body weight of the mice after virus challenge. (A) Survival rate of the mice after HK483 challenge. Groups of mice were immunised H5 vaccine intranasally with CTB*, poly (I:C), CMP or poly (I:C) + CMP as an adjuvant and infected intranasally with 100 LD_{50} of HK483 virus suspension. (B) Changes in body weight of mice after virus challenge in the same groups as in Fig. 3A. Each point represents the mean of the relative ratio for initial body weight of 5 mice on each day.

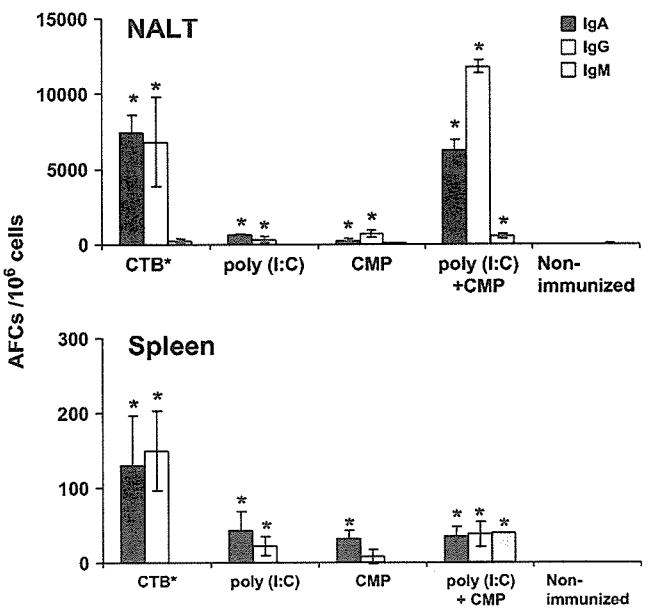

Fig. 4. ELISPOT assay of lymphocytes from the NALT and spleen of mice immunised with H5 vaccine with CTB*, poly (I:C), CMP or poly (I:C) + CMP as an adjuvant. The H5-HA protein-specific AFCs were enumerated by ELISPOT assay. The value were compared statistically with those of non-immunised mice with the *t*-test for paired observations. $*p < 0.05$.

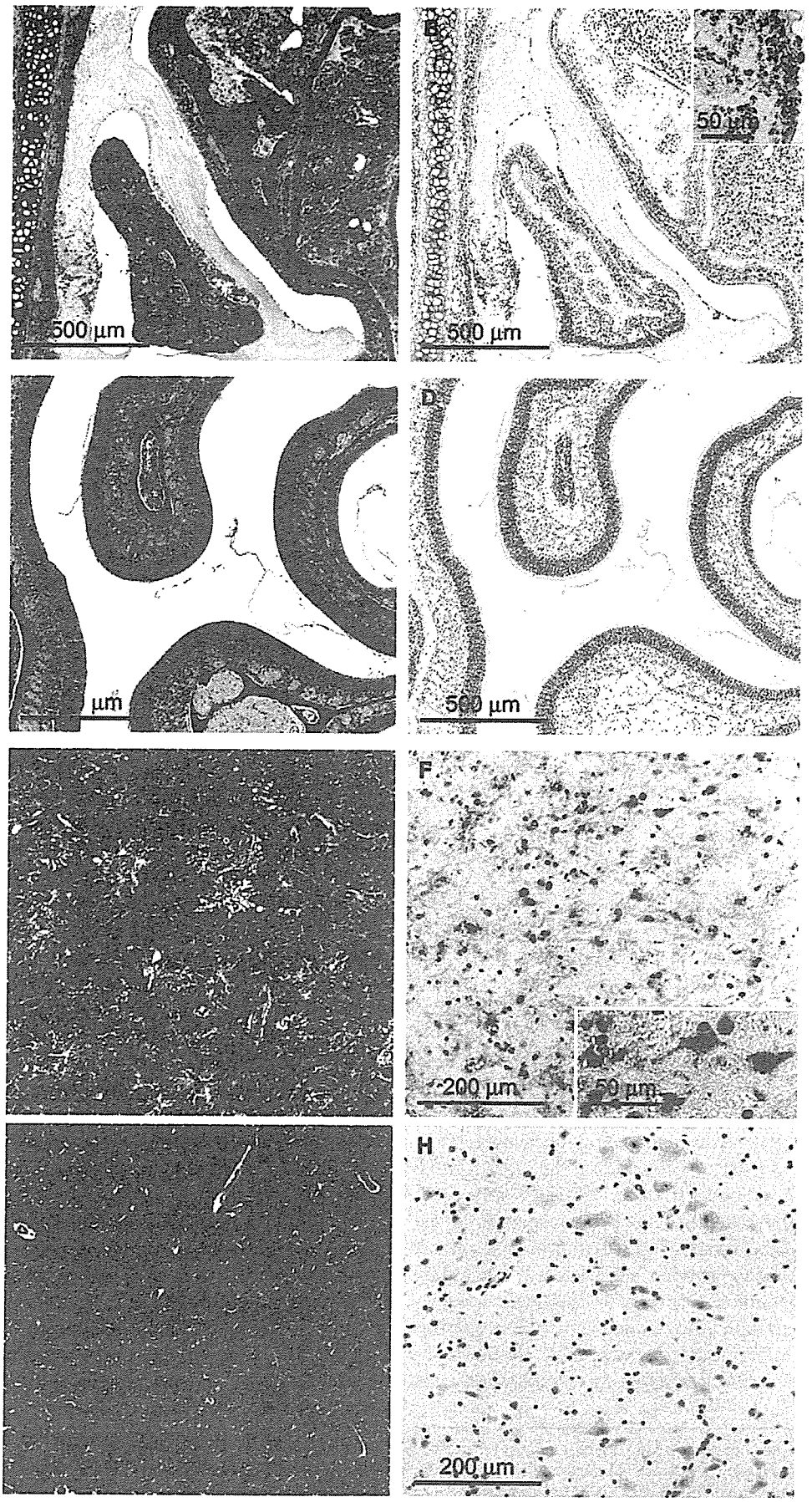
500 μm
B
500 μm
50 μm
μm
D
500 μm
F
200 μm
50 μm
H
200 μm